J|A|C|S
ARTICLES
Published on Web 12/05/2006

Driven Evolution of a Constitutional Dynamic Library of Molecular Helices Toward the Selective Generation of [2 × 2] Gridlike Arrays under the Pressure of Metal Ion Coordination

Nicolas Giuseppone, Jean-Louis Schmitt, and Jean-Marie Lehn*

Contribution from the Laboratoire de Chimie Supramoléculaire, Institut de Science et d'Ingénierie Supramoléculaires, Université Louis Pasteur, 8 Allée Gaspard Monge, BP 70028, 67083 Strasbourg Cedex, France

Received October 5, 2006; E-mail: lehn@isis.u-strasbg.fr

Abstract: Constitutional dynamics, self-assembly, and helical-folding control are brought together in the efficient $Sc(OTf)_3$/microwave-catalyzed transimination of helical oligohydrazone strands, yielding highly diverse dynamic libraries of interconverting constituents through assembly, dissociation, and exchange of components. The transimination-type mechanism of the Sc^{III}-promoted exchange, as well as its regioselectivity, occurring only at the extremities of the helical strands, allow one to perform directional terminal polymerization/depolymerization processes when starting with dissymmetric strands. A particular library is subsequently brought to express quantitatively [2 × 2] gridlike metallosupramolecular arrays in the presence of Zn^{II} ions by component recombination generating the correct ligand from the dynamic set of interconverting strands. This behavior represents a process of driven evolution of a constitutional dynamic chemical system under the pressure (coordination interaction) of an external effector (metal ions).

Introduction

Molecular and supramolecular self-organization results from programmed structure generation directed by conformational properties and intermolecular noncovalent interactions.[1−3] The functions carried out by biological macromolecules, for example, nucleic acids and proteins, are based on their ability to perform processes such as molecular recognition and catalysis, via well-defined three-dimensional (supra)-molecular interactions. In particular, internal folding of molecular strands in biological helical structures is induced by well-defined long-range interactions.[4,5] In view of its significance in biology, the precise generation and control of folded entities capable of mimicking the secondary structures of such biopolymers has been intensively studied. Furthermore, artificial self-organized structures can be implemented in catalysis, materials science, or nanotechnologies, and numerous investigations have recently been directed toward these domains by various research groups.[6] Typically, the generation of synthetic helical species may be enforced through the implementation of "helicity codons"[7] based on nonbonded interactions within specific polyheterocyclic strands,[7,8] or on noncovalent interactions such as hydrogen bonding[9,10] or metal−ligand coordination.[6a,11] In particular, the construction of helical strands by condensation of suitably designed hydrazino and carbonyl components into reversible hydrazone type bonds gives access to dynamic libraries of molecular helices.[12,13]

(1) Lehn, J.-M. *Supramolecular Chemistry − Concepts and Perspectives*; VCH: Weinheim, 1995.
(2) Lehn, J.-M. *Chem.-Eur. J.* **2000**, *6*, 2097.
(3) Lehn, J.-M. *Proc. Natl. Acad. Sci. U.S.A.* **2002**, *99*, 4763.
(4) Mirsky, A. E.; Pauling, L. *Proc. Natl. Acad. Sci. U.S.A.* **1936**, *22*, 439. Bränden, C.; Tooze, J. *Introduction to Protein Structure*; Garland: New York, 1991.
(5) Special Issue on Protein Folding. *Acc. Chem. Res.* **1998**, *31*, 697.
(6) For review articles, see: (a) Piguet, C.; Bernardinelli, G.; Hopfgartner, G. *Chem. Rev.* **1997**, *97*, 2005. (b) Rowan, A. E.; Nolte, R. J. M. *Angew. Chem.* **1998**, *112*, 65; *Angew. Chem., Int. Ed.* **1998**, *37*, 63. (c) Hill, D. J.; Mio, M. J.; Prince, R. B.; Hughes, T. S.; Moore, J. S. *Chem. Rev.* **2001**, *101*, 3893. (d) Huc, I. *Eur. J. Org. Chem.* **2004**, 17.
(7) Ohkita, M.; Lehn, J.-M.; Baum, G.; Fenske, D. *Chem.-Eur. J.* **1999**, *5*, 3471.
(8) (a) Hanan, G. S.; Lehn, J.-M.; Kyritsakas, N.; Fischer, J. *J. Chem. Soc., Chem. Commun.* **1995**, 765. (b) Hanan, G. S.; Schubert, U. S.; Volkmer, D.; Riviere, E.; Lehn, J.-M.; Kyritsakas, N.; Fischer, J. *Can. J. Chem.* **1997**, *75*, 169. (c) Bassani, D. M.; Lehn, J.-M.; Baum, G.; Fenske, D. *Angew. Chem., Int. Ed. Engl.* **1997**, *36*, 1845. (d) Bassani, D. M.; Lehn, J.-M. *Bull. Soc. Chim. Fr.* **1997**, *134*, 897. (e) Cuccia, L. A.; Lehn, J.-M.; Homo, J.-C.; Schmutz, M. *Angew. Chem., Int. Ed.* **2000**, *39*, 233. (f) Cuccia, L. A.; Ruiz, E.; Lehn, J.-M.; Homo, J.-C.; Schmutz, M. *Chem.-Eur. J.* **2002**, *8*, 3448. (g) Petitjean, A.; Cuccia, L. A.; Lehn, J.-M.; Nierengarten, H.; Schmutz, M. *Angew. Chem., Int. Ed.* **2002**, *41*, 1195.
(9) (a) Gellman, S. H. *Acc. Chem. Res.* **1998**, *31*, 173. (b) Stigers, K. D.; Soth, M. J.; Nowick, J. S. *Curr. Opin. Chem. Biol.* **1999**, *3*, 714. (c) Gong, B. *Chem.-Eur. J.* **2001**, *7*, 4337. (d) Seebach, D.; Schriber, J. V.; Arvidsson, P. I.; Frackenpohl, J. *Helv. Chim. Acta* **2001**, *84*, 271. (e) Gee, P. J.; Hamprecht, F. A.; Schuler, L. D.; van Gunsteren, W. F.; Duchardt, E.; Schwalbe, H.; Albert, M.; Seebach, D. *Helv. Chim. Acta* **2002**, *85*, 618. (f) Yang, D.; Zhang, Y.-H.; Zhu, N.-Y. *J. Am. Chem. Soc.* **2002**, *124*, 9966.
(10) (a) Berl, V.; Huc, I.; Khoury, R. G.; Krische, M.; Lehn, J.-M. *Nature* **2000**, *407*, 720. (b) Berl, V.; Huc, I.; Khoury, R. G.; Lehn, J.-M. *Chem.-Eur. J.* **2001**, *7*, 2798. (c) Berl, V.; Huc, I.; Khoury, R. G.; Lehn, J.-M. *Chem.-Eur. J.* **2001**, *7*, 2810.
(11) (a) Lehn, J.-M.; Rigault, A.; Siegel, J.; Harrowfield, J.; Chevrier, B.; Moras, D. *Proc. Natl. Acad. Sci. U.S.A.* **1987**, *84*, 2565. (b) Wu, P.; Janiak, C.; Uehlin, L.; Klüfers, P.; Mayer, P. *Chem. Commun.* **1998**, 2637. Baum, G.; Constable, E. C.; Fenske, D.; Housecroft, C. E.; Kulke, T. *Chem. Commun.* **1999**, 195. (c) Norsten, T. B.; McDonald; Branda, N. R. *Chem. Commun.* **1999**, 719. (d) Hannon, M. J.; Painting, C. L.; Alcock, N. W. *Chem. Commun.* **1999**, 2023. (e) Calder, D. L.; Raymond, K. R. *Acc. Chem. Res.* **1999**, *32*, 975. (f) Albrecht, M. *J. Inclusion Phenom. Macrocycl. Chem.* **2000**, *36*, 127.
(12) (a) Gardinier, K. M.; Khoury, R. G.; Lehn, J.-M. *Chem.-Eur. J.* **2000**, *22*, 4124. (b) Schmitt, J.-L.; Stadler, A.-M.; Kyritsakas, N.; Lehn, J.-M. *Helv. Chim. Acta* **2003**, *86*, 1598. (c) Schmitt, J.-L.; Lehn, J.-M. *Helv. Chim. Acta* **2003**, *86*, 3417.
(13) For the folding-driven synthesis of imine oligomers, see: Oh, K.; Jeong, K.-S.; Moore, J. S. *Nature* **2001**, *414*, 889. Zhao, D.; Moore, J. S. *J. Am. Chem. Soc.* **2003**, *125*, 16294.

10.1021/ja0666452 CCC: $33.50

Constitutional dynamic chemistry (CDC)[3,14] encompasses the study of the dynamic features presented by the constitution of molecular[15,16] as well as supramolecular[17] entities linked through reversible connections. The generation of constitutional diversity by exchange and reshuffling of components is by essence subjected to evolution under the pressure of molecular information and recognition processes. This seminal concept has been implemented in particular in the recently developed dynamic combinatorial/covalent chemistry (DCC).[16] Basically, in dynamic combinatorial/covalent libraries (DCLs), the thermodynamic equilibrium may be shifted toward the amplification of the substrate best-fitted for a given receptor through host−guest recognition. Numerous investigations have been pursued on DCC by different research groups over the past decade, highlighting its potentialities in the field of drug discovery[18] as well as in the self-assembly of molecular receptors[19,20a,b] and of metallosupramolecular architectures.[20] In recent years, work from our laboratory has shown that these basic principles can be implemented in materials science and has extended the range of suitable external triggers to pH,[21,22b] metal ions,[22] temperature,[21] the formation of a stable hydrogel[23a] or of a solid,[23b] application of an electric field,[24] and by tuning the physical properties of dynamic polymers, dynamers,[14b,25] upon controlling their constitution with external stimuli.[22]

The key to the generation of dynamic constitutional diversity for both biological and materials science purposes resides in the availability of chemical connections displaying efficient reversibility in a given set of (mild) conditions. The C═N unit, present in imines, hydrazones, and oximes, offers in principle highly attractive potentialities to CDC, provided fast reversibility in organic solvents is achieved. We have recently described the Lewis acid catalysis of self-sufficient transimination reactions using $Sc(OTf)_3$ in organic solvents with accelerations of over 10^5 as compared to the uncatalyzed pathway.[26] This methodology was applied to the generation of a constitutional dynamic library of helical strands incorporating hydrazone bonds and capable of assembling, dissociating, and exchanging components. We also demonstrated that this library can undergo driven evolution in the presence of suitable metal ions, that is, Zn(II) salts, to express preferentially [2 × 2] grid-type metal complexes from the mixture of helices. These combined processes are illustrated schematically in Figure 1.[27]

We here present a detailed account of these preliminary results. First, we show that the exchanges promoted by Sc^{III} ions can be highly accelerated upon microwave activation due to a local heating of the catalyst. Second, we point out that the mechanism of the constitutional exchange involves interesting directionally polarized polymerization/depolymerization processes. Finally, we highlight an optimized DCC system in which a library of helices can be driven to full reorganization toward the formation of [2 × 2] grid-type complexes.

Results and Discussion

I. Synthesis and Conformational Analysis of the Building Blocks. Previous investigations in our laboratory have established the helical structure of molecular strands based on pyrimidine−pyridine−pyrimidine (*pym*−*py*−*pym*) sequences (Scheme 1, **A**).[7,8] In these units, the helicity is enforced by the programmed intramolecular self-organization carried out by three encoding features: (1) an alternating *pym*−*py*−*pym* sequence, (2) linkages at specific positions, and (3) the strong preference for the transoid conformation around the single bonds between the α,α′-linked heterocyclic units. Nevertheless, syn-

(14) (a) Lehn, J.-M. *Science* **2002**, *295*, 2400. (b) Lehn, J.-M. *Prog. Polym. Sci.* **2005**, *30*, 814.

(15) Rowan, S. J.; Cantrill, S. J.; Cousins, G. R. L.; Sanders, J. K. M.; Stoddart, J. F. *Angew. Chem.* **2002**, *114*, 938; *Angew. Chem., Int. Ed.* **2002**, *41*, 898.

(16) (a) Lehn, J.-M. *Chem.-Eur. J.* **1999**, *5*, 2455. (b) Cousins, R. L.; Poulsen, S. A.; Sanders, J. K. M. *Curr. Opin. Chem. Biol.* **2000**, *4*, 270. (c) Corbett, P. T.; Leclaire, J.; Vial, J.; West, K. R.; Wietor, J.-L.; Sanders, J. K. M.; Otto, S. *Chem. Rev.* **2006**, *106*, 3652.

(17) Lehn, J.-M. In *Supramolecular Science: Where It Is and Where It Is Going*; Ungaro, R., Dalcanale, E., Eds.; Kluwer: Dordrecht, The Netherlands, 1999; p 287.

(18) (a) Swann, P. G.; Casanova, R. A.; Desai, A.; Frauenhoff, M. M.; Urbanic, M.; Slomezynska, U.; Hopfinger, A. J.; Le, Breton, G. C.; Venton, D. L. *Biopolymers* **1996**, *40*, 617. (b) Huc, I.; Lehn, J.-M. *Proc. Natl. Acad. Sci. U.S.A.* **1997**, *94*, 2106. (c) Eliseev, A.; Nelen, M. *J. Am Chem. Soc.* **1997**, *119*, 1147. (d) Ramström, O.; Lehn, J.-M. *ChemBioChem* **2000**, *1*, 41. (e) Nicolaou, K. C.; Hughes, R.; Cho, S. Y.; Winssinger, N.; Smethurst, C.; Labischinski, H.; Endermann, R. *Angew. Chem.* **2000**, *112*, 3981; *Angew. Chem., Int. Ed.* **2000**, *39*, 3823. (f) Case, M. A.; McLendon, G. L. *J. Am. Chem. Soc.* **2000**, *122*, 8089. (g) Bunyapaiboonsri, T.; Ramström, O.; Lohmann, S.; Lehn, J.-M.; Peng, L.; Goeldner, M. *ChemBioChem* **2001**, *2*, 438. (h) Hochgürtel, M.; Kroth, H.; Piecha, D.; Hofmann, M. W.; Nicolau, C.; Krause, S.; Schaaf, O.; Sonnenmoser, G.; Eliseev, A. V. *Proc. Natl. Acad. Sci. U.S.A.* **2002**, *99*, 3382. (i) Lins, R. J.; Flitsch, S. L.; Turner, N. J.; Irving, E.; Brown, S. A. *Angew. Chem.* **2002**, *114*, 3555; *Angew. Chem., Int. Ed.* **2002**, *41*, 3405. (j) Gerber-Lemaire, S.; Popowycz, F.; Rodríguez-García, E.; Carmona, Asenjo, A. T.; Robina, I.; Vogel, P. *ChemBioChem* **2002**, *5*, 466. (k) Hochgürtel, M.; Biesinger, R.; Kroth, H.; Piercha, D.; Hofmann, M. W.; Krause, S.; Schaaf, O.; Nicolau, C.; Eliseev, A. V. *J. Med. Chem.* **2003**, *46*, 356. (l) Ramström, O.; Lohmann, S.; Bunyapaiboonsri, T.; Lehn, J.-M. *Chem.-Eur. J.* **2004**, *10*, 1711. (m) Zameo, S.; Vauzeilles, B.; Beau, J.-M. *Angew. Chem.* **2005**, *117*, 987; *Angew. Chem., Int. Ed.* **2005**, *44*, 965.

(19) (a) Cousins, G. R. L.; Furlan, R. L. E.; Ng, Y.-F.; Redman, J. E.; Sanders, J. K. M. *Angew. Chem.* **2001**, *113*, 437; *Angew. Chem., Int. Ed.* **2001**, *40*, 423. (b) Otto, S.; Furlan, R. L. E.; Sanders, J. K. M. *Curr. Opin. Chem. Biol.* **2002**, *6*, 321. (c) Furlan, R. L. E.; Ng, Y.-F.; Otto, S.; Sanders, J. K. M. *J. Am. Chem. Soc.* **2001**, *123*, 8876. (d) Otto, S.; Furlan, R. L. E.; Sanders, J. K. M. *Science* **2002**, *297*, 590. (e) Roberts, S. L.; Furlan, R. L. E.; Cousins, G. R. L.; Sanders, J. K. M. *Chem. Commun.* **2002**, 938. (f) Otto, S.; Kubik, S. *J. Am. Chem. Soc.* **2003**, *125*, 7804.

(20) For inorganic entities, see, for instance: (a) Hasenknopf, B.; Lehn, J.-M.; Kneisel, B. O.; Baum, G.; Fenske, D. *Angew. Chem.* **1996**, *108*, 1987; *Angew. Chem., Int. Ed. Engl.* **1996**, *35*, 1838. (b) Hasenknopf, B.; Lehn, J.-M.; Boumediene, N.; Dupont-Gervais, A.; Van, Dorsselaer, A.; Kneisel, B.; Fenske, D. *J. Am. Chem. Soc.* **1997**, *119*, 10956. (c) Fleming, J. S.; Mann, K. L. V.; Carraz, C.-A.; Psillakis, E.; Jeffery, J. C.; McCleverty, J. A.; Ward, M. D. *Angew. Chem.* **1998**, *110*, 1315; *Angew. Chem., Int. Ed.* **1998**, *37*, 1279. (d) Huc, I.; Krische, M. J.; Funeriu, D. P.; Lehn, J.-M. *Eur. J. Inorg. Chem.* **1999**, 1415. (e) Goral, V.; Nelen, M. I.; Eliseev, A. V.; Lehn, J.-M. *Proc. Natl. Acad. Sci. U.S.A.* **2001**, *98*, 1347. (f) Johnson, D. W.; Raymond, K. N. *Inorg. Chem.* **2001**, *40*, 5157. (g) Grote, Z.; Scopelliti, R.; Severin, K. *Angew. Chem., Int. Ed.* **2003**, *42*, 3821. (h) Mezei, G.; Baran, P.; Raptis, R. G. *Angew. Chem.* **2004**, *116*, 584; *Angew. Chem., Int. Ed.* **2004**, *43*, 574. (i) Huang, X.-C.; Zhang, J.-P.; Chen, X.-M. *J. Am. Chem. Soc.* **2004**, *126*, 13218. (j) Aoyagi, M.; Minamikawa, H.; Shimizu, T. *Chem. Lett.* **2004**, *33*, 860. (k) Mahmoudkhani, A. H.; Côté, A. P.; Shimizu, G. K. H. *J. Chem. Soc., Chem. Commun.* **2004**, 2678. (l) Brumaghim, J. L.; Michels, M.; Raymond, K. N. *Eur. J. Org. Chem.* **2004**, 4554. (m) Chi, K.-W.; Addicott, C.; Arif, A. M.; Stang, P. J. *J. Am. Chem. Soc.* **2004**, *126*, 16569. (n) Saur, I.; Scopelliti, R.; Severin, K. *Chem.-Eur. J.* **2006**, *12*, 1058. (o) Storm, O.; Lüning, U. *Chem.-Eur. J.* **2002**, *8*, 793.

(21) (a) Giuseppone, N.; Lehn, J.-M. *Chem.-Eur. J.* **2006**, *12*, 1715. (b) For the influence of pH and temperature on dynamic covalently bonded rotaxanes, see: Kawai, H.; Umehara, T.; Fujiwara, K.; Tsuji, T.; Suzuki, T. *Angew. Chem.* **2006**, *118*, 4387; *Angew. Chem., Int. Ed.* **2006**, *45*, 4281.

(22) (a) Giuseppone, N.; Lehn, J.-M. *J. Am. Chem. Soc.* **2004**, *126*, 11448. (b) Giuseppone, N.; Fuks, G.; Lehn, J.-M. *Chem.-Eur. J.* **2006**, *12*, 1723.

(23) (a) Nampally, S.; Lehn, J.-M. *Proc. Natl. Acad. Sci. U.S.A.* **2005**, *102*, 5938. (b) For an earlier example, concerning a constitutional reorganization of equilibrating coordination compounds driven by crystallization, see: Baxter, P. N. W.; Lehn, J.-M.; Rissanen, K. *J. Chem. Soc., Chem. Commun.* **1997**, 1323. (c) By solvent composition, see: Baxter, P. N. W.; Khoury, R. G.; Lehn, J.-M.; Baum, G.; Fenske, D. *Chem.-Eur. J.* **2000**, *6*, 4140.

(24) Giuseppone, N.; Lehn, J.-M. *Angew. Chem.* **2006**, *118*, 4735; *Angew. Chem., Int. Ed.* **2006**, *45*, 4616.

(25) The term "dynamers" designates dynamic polymers connected by either reversible covalent or non-covalent bonds: (a) Lehn, J.-M. *Polym. Int.* **2002**, *51*, 825. (b) Polyacylhydrazones: Skene, W. G.; Lehn, J.-M. *Proc. Natl. Acad. Sci. U.S.A.* **2004**, *101*, 8270. (c) *Supramolecular Polymers*, 2nd ed.; Ciferri, A., Ed.; Taylor Francis: New York, 2004.

(26) Giuseppone, N.; Schmitt, J.-L.; Schwartz, E.; Lehn, J.-M. *J. Am. Chem. Soc.* **2005**, *127*, 5528 and references therein.

(27) Giuseppone, N.; Schmitt, J.-L.; Lehn, J.-M. *Angew. Chem.* **2004**, *116*, 5010; *Angew. Chem., Int. Ed.* **2004**, *43*, 4902.

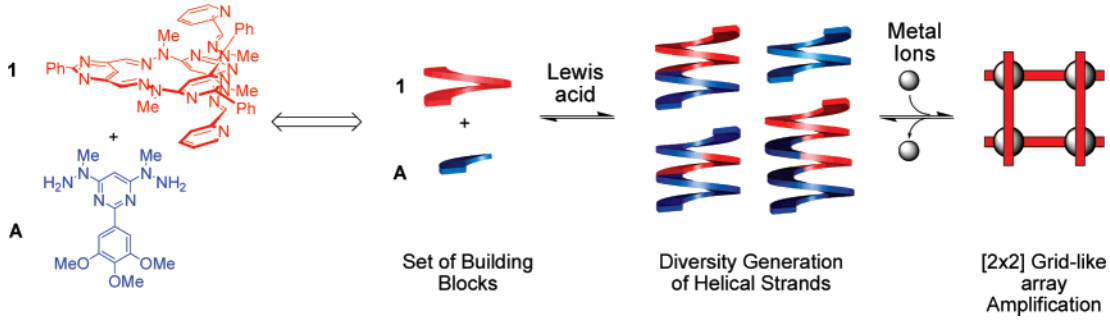

Figure 1. Schematic representation of the constitutional dynamic processes undergone by the present system: (left) Lewis acid-catalyzed generation of dynamic constitutional diversity in helical molecular strands, involving compounds **1** and **A**, with **1** shown in its preferred helical folding; (right) evolution of the dynamic library toward the formation of a [2 × 2] grid driven by the coordination of suitable metal ions.[27]

Scheme 1. Schematic Representation of the Isomorphic Correspondence between the Helicity Codons *pym*−*py*−*pym* (Sequence **A**), and *pym*−*hyz*−*pym* (Sequence **B**), Represented in Their Transoid Form[a]

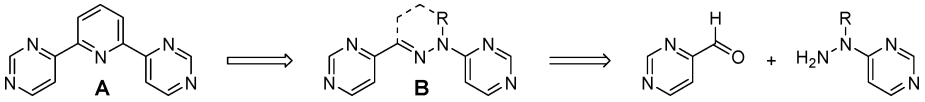

[a] One helical turn is constituted of three of the represented units **A** and **B** and enforced by (1) the electrostatic repulsion between the nitrogen dipoles, (2) the steric repulsion between the CH's in the cisoid conformation, and (3) the presence of weak CH···N hydrogen bondings in the transoid form.[12]

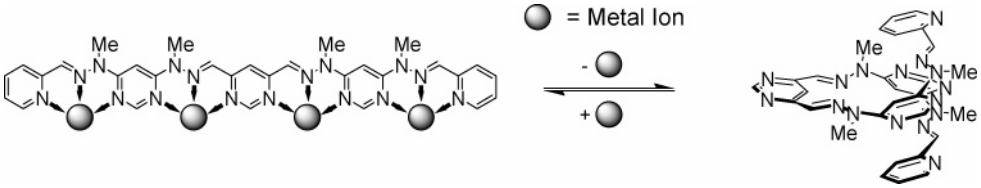

Figure 2. Schematic representation of the conformational dynamic folding/unfolding of *hyz*−*pym*-based chains, triggered by metal ion binding.[28]

thetic access to such helicity codons necessitates extensive synthetic efforts. The isomorphic correspondence between the *py* group of the *pym*−*py*−*pym* sequence and a hydrazone (*hyz*) group provides a powerful alternative approach and greatly simplifies the connection of building blocks by making use of the hydrazone condensation reaction (Scheme 1, right). Molecular strands built on several hydrazone−pyrimidine (*hyz*−*pym*) units indeed undergo self-organization into helices both in solution and in the solid state, as has been shown by NMR spectroscopy and X-ray crystallography.[12]

In addition to their easy accessibility from simple condensation of the corresponding hydrazine and aldehyde moieties and to their preferential helical folding, the *hyz*−*pym* sequences present two types of dynamic features: motional dynamic processes, conformational changes triggered by metal-ion binding and allowing contraction/extension motions, that is, reversible folding/unfolding into helical/linear shapes (Figure 2);[28] and constitutional dynamic processes resulting from the well-established reversibility of the hydrazone[29] connection and involving component exchange, reorganization, incorporation, and decorporation as well as chain lengthening or shortening (Figure 1).

To study the constitution of the dynamic libraries of helical strands and to accurately identify their members, we first synthesized a series of building blocks as well as some more advanced intermediates that may be involved in the generation of combinatorial diversity through dynamic reshuffling (Figure 3). The general synthetic pathways to access these monomeric and oligomeric entities have been published elsewhere,[12b,c] and the new compounds are described in the Experimental Section.

II. Generation of Dynamic Constitutional Diversity. Helicity-encoded oligomeric and polymeric molecular strands based on hydrazone connections have been found to resist many attempts to perform component exchange,[12b] indicating a high stability even at an elevated temperature and/or in the presence of acid. As model systems for the exploration of potential exchange catalysts, crossover experiments between the dihydrazone compound **5** and the dihydrazine **A** in chloroform at 60 °C were performed first (Figure 4). In these conditions and without a catalyst, only 7% of **5** had been consumed after 48 h and slow degradation of constituents of the mixture had taken place. Under acid catalysis (20 mol % CF_3CO_2H), extensive decomposition into unidentified compounds other than **2**−**4**, **B** occurred. In contrast, addition of 20 mol % of $Zn(BF_4)_2 \cdot H_2O$[22b] led to complete exchange with a half-life time of 10 h without observable degradation (Figure 4a). With $Sc(OTf)_3$ as a catalyst, the exchange is very efficient and the equilibrium is reached with a half-life time of only 20 min (30 times faster) (Figure 4b). The statistical distribution of the products at equilibrium indicates the nonspecific interaction of the metal ions with the different compounds and the isoenergetic nature of the library.[16a] As in the case of other C═N bonds under Sc^{III} catalysis,[26] the reaction proceeds via a transimination process; indeed, in similar conditions, the pyrimidine 4,6-biscarboxaldehyde analogue of **B** and dihydrazone **5** did not yield any detectable amount of exchange after 3 days. Moreover, for the lanthanide triflate series

(28) Stadler, A.-M.; Kyritsakas, N.; Graff, R.; Lehn, J.-M. *Chem.-Eur. J.* **2006**, *12*, 4503.
(29) Katritzky, A. R.; Meth-Cohn, O.; Rees, C. W. *Comprehensive Organic Functional Group Transformations*; Pergamon: New York, 1995; Vol. 3, p 404.
(30) In all structural formulas, the molecules are shown, for clarity, in a linear, extended representation rather than in the correct helical form.

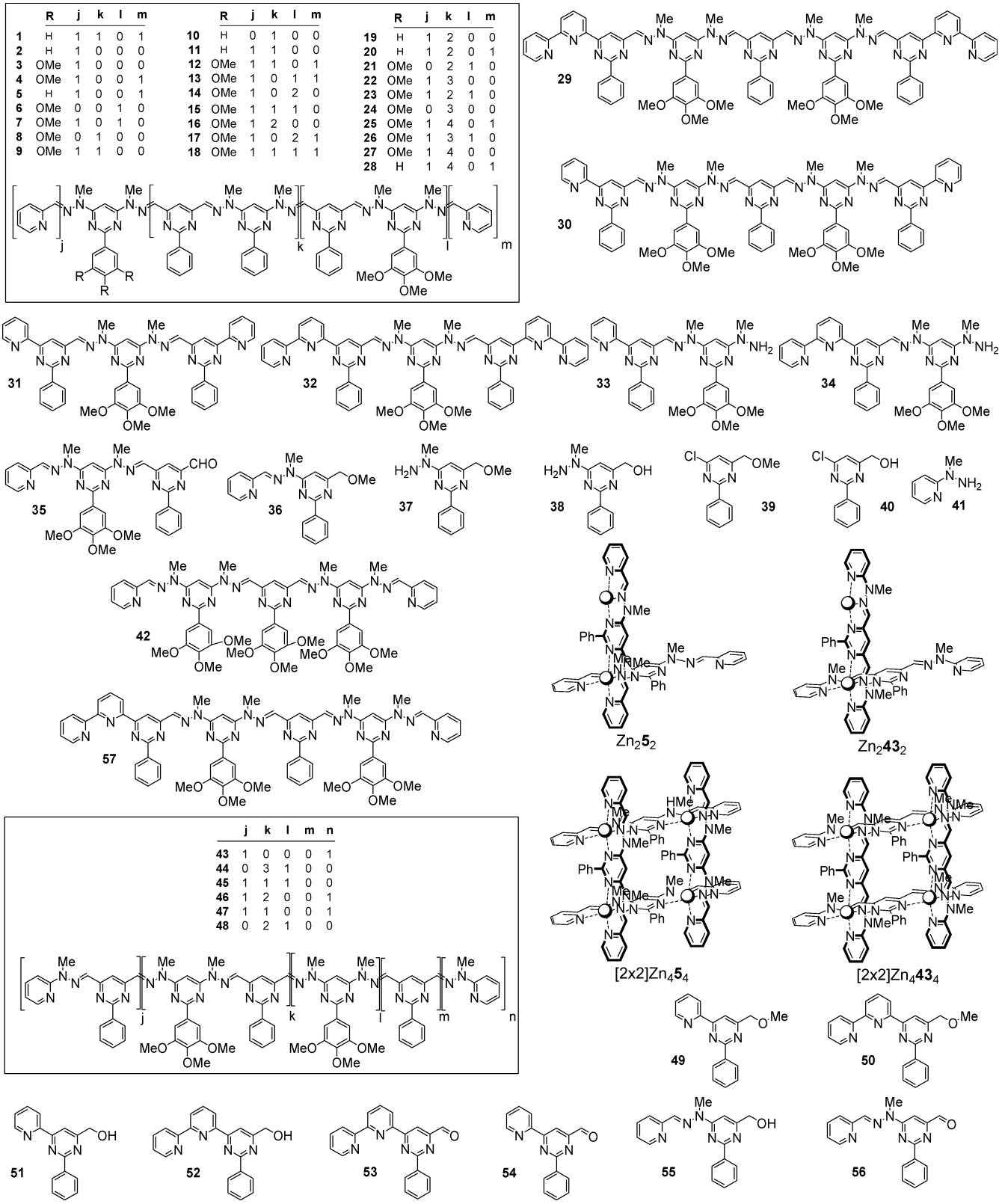

Figure 3. Structures of the compounds contained in the dynamic libraries investigated. Compounds **1**−**5**, **12**, **13**, **20**, **29**−**43**, **49**−**57**, as well as the two grid structures [2 × 2]Zn$_4$**5**$_4$ and [2 × 2]Zn$_4$**43**$_4$ were synthesized and characterized as described.[12a,b,30,33]

(Sc, Yb, Y, Sm, and La), the results indicated that the activity was directly correlated with the ionic radius of the trivalent metallic ions assayed, with scandium being the most powerful Lewis acid catalyst for hydrazone scrambling, in agreement with earlier results.[26]

To test the efficiency and generality of the process, we moved to compound **1**, a 1-turn helical strand containing four hydrazone groups, which was expected to be much more reluctant to undergo component exchange (Figure 5, equilibrium (a)) than the shorter related structures (**2**−**5**, Figure 3), due to its folding

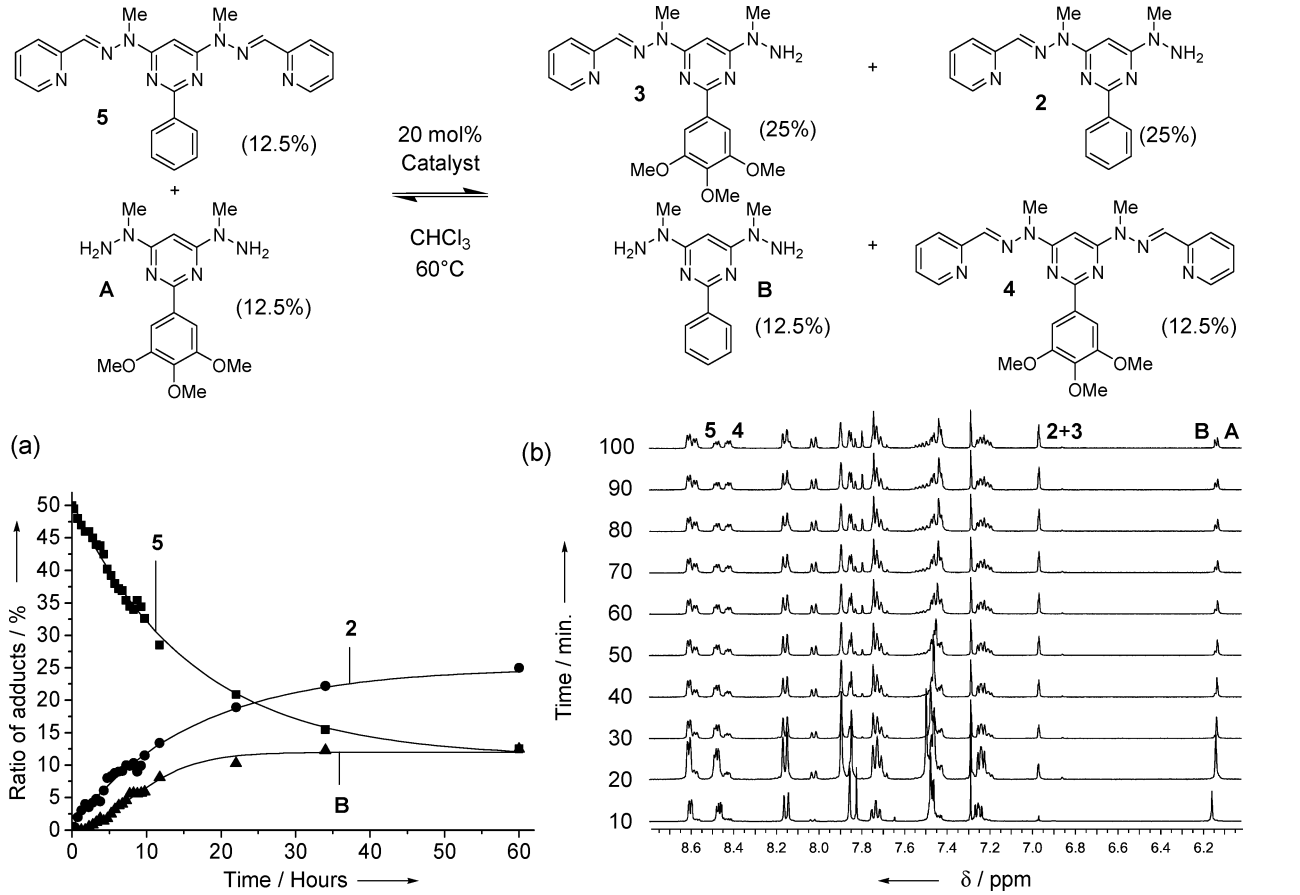

Figure 4. Evolution with time of the composition of the hydrazone/hydrazine mixture **5**, **A** as model reaction for component exchange (top): followed by ^{1}H NMR (a) under Zn^{II} catalysis and (b) under Sc^{III} catalysis; c(**5**) = c(**A**) = 50 mm.[30]

and the resulting lesser accessibility of its hydrazone sites (vide infra). Compound **1** nevertheless underwent exchange of its two bis-hydrazine components with bis-hydrazine **A** in 48 h when mixed in a stoichiometric ratio in the presence of 20 mol % (i.e., 5 mol % per hydrazone site of **1**) of $Sc(OTf)_3$ in chloroform at 60 °C. The equilibrium was reached after about 48 h as indicated by the stabilized pattern of the complex ^{1}H NMR spectra (Figure 5, top right). Even with only 4% catalyst (i.e., 1% per site), extensive exchange had taken place after 48 h, although the reaction was much slower. The constituents of the mixture could be separated and identified by HPLC/ESMS (Figure 5, bottom). The data analysis demonstrated that full recombination between **1** and **A** had taken place, with the generation of the set of compounds **1**−**28**, containing even expanded helices of up to 10 hydrazone sites (more than 3 helical turns). Moreover, all of the possible cross-combinations with components bearing phenyl and/or methoxyphenyl moieties were statistically generated for each size of helical strand (Gaussian distribution), highlighting the efficiency of the reorganization process.

III. Activation by Microwave Heating. To further improve the efficiency of the Sc^{III} scrambling catalysis, we investigated the potential effect of activation by microwave heating on the equilibration rate of another model system involving hydrazone **36** and bis-hydrazinopyrimidine **A** in deuterated tetrachloroethane (Figure 6, top). In this mixture, the application of microwave heating at a constant temperature of 140 °C enables one to reach the equilibrium after only 4 min, while it requires 12 min under oil bath heating (Figure 6, bottom left). Without a catalyst, the microwave irradiation at 140 °C produces only 5% of conversion after 1 h (measured in ^{1}H NMR by the decrease of **36**). The graphical representation of the systematic comparison between classical heating (Figure 6, bottom right, squares) and microwave heating (dots) for various temperatures between 60 and 200 °C shows the linear dependence of both processes on the temperature. Besides, the steep slope observed under microwave irradiation could be indication for a very efficient local heating of the metal center, leading to an improvement of its efficiency as a catalyst.

Finally, microwave activation does not generate detectable degradation products even in more complex systems, and the equilibrium involving helices described in Figure 5 can be reached in only 30 min at 140 °C in $C_2D_2Cl_4$, as compared to the 48 h necessary previously. It should also be pointed out that the use of microwaves is compatible with grid-type metal complexes, as it does not disrupt their coordination structures (vide infra).

IV. Mechanistic Aspects of the Exchange Process − Toward Directionally Polarized Polymerization/Depolymerization Processes. The mechanism of catalyzed transimination in organic solvents was investigated previously, and, in most cases, rate accelerations were higher with Sc^{III} ions as compared to those with protons.[26] It was, however, unexpected that for the equilibration described in Figure 5 and under Brönsted acid catalysis (20 mol % CF_3CO_2H) after 48 h, only traces of **1** had been converted solely into compounds **11** and **3** and degradation of the dihydrazine **A** had set in (as shown by NMR and LC/MS).[31] Therefore, in the particular case of *hyz*−*pym*-based

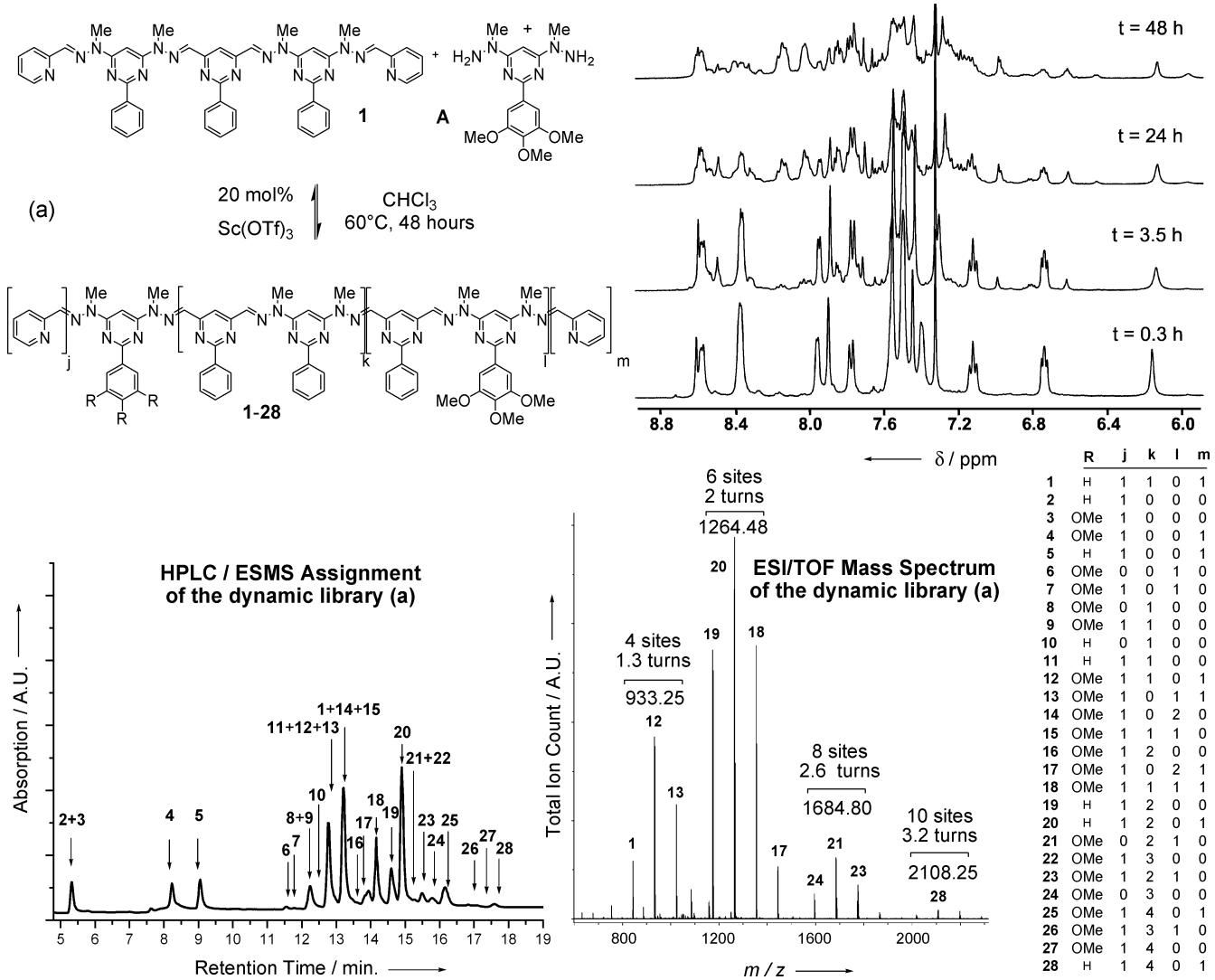

	R	j	k	l	m
1	H	1	1	0	1
2	H	1	0	0	0
3	OMe	1	0	0	0
4	OMe	1	0	0	1
5	H	1	0	0	1
6	OMe	0	0	1	0
7	OMe	1	0	1	0
8	OMe	0	1	0	0
9	OMe	1	1	0	0
10	H	0	1	0	0
11	H	1	1	0	0
12	OMe	1	1	0	1
13	OMe	1	0	1	1
14	OMe	1	0	2	0
15	OMe	1	1	1	0
16	OMe	1	2	0	0
17	OMe	1	0	2	1
18	OMe	1	1	1	1
19	H	1	2	0	0
20	H	1	2	0	1
21	OMe	0	2	1	0
22	OMe	1	3	0	0
23	OMe	1	2	1	0
24	OMe	0	3	0	0
25	OMe	1	4	0	1
26	OMe	1	3	1	0
27	OMe	1	4	0	0
28	H	1	4	0	1

Figure 5. Generation of a highly diverse recombination library of helicity-encoded molecular strands from the 1-turn/4-sites helical compound **1** ($c = 50$ mm) and the dihydrazine **A** ($c = 50$ mm) using $Sc(OTf)_3$ (20%) as catalyst in $CDCl_3$ at 60 °C; ^1H NMR spectra show the evolution of the equilibrium with time and its stabilization after 48 h (top right); 28 constituents have been identified by LC/MS (bottom left) and direct introduction ESI/TOF (bottom center) mass spectrometry, as indicated (bottom right).[30]

helical strands, Sc^{III} acts as an efficient promoter of the exchange. Insight into this specific behavior can be gained from the crystal structures of protonated and non-protonated *hyz*−*pym* sequences of various lengths (Figure 7).

The solid-state molecular structure of compound **42**, a 4 hydrazone sites/1-turn helical strand, shows that access to the exchangeable C═N bonds is hindered by wrapping of the molecule around them, thus leading to a low reactivity for the transimination reaction (Figure 7). The activation of the hydrazone sites would require an unfolding via a change of the *s-trans* to the *s-cis* conformation through, for example, chelation to a cationic center. However, protonation does not lead to an unfolding of such structures. Indeed, the crystal structure of the diprotonated form of **43** (Figure 7) shows that the two protons are located on the pyridine moieties and do not lead to the desired *s-cis* linear strand. A similar observation was also made for the crystal structure of the bis-protonated helical strand of **1**, although the resolution of the structure was of low quality (data not shown). On the other hand, it is known that Zn^{II} and Pb^{II} ions are able to fully unfold helical strands based on *hyz*−*pym* sequences and produce racks of linear shape (see Figure 2).[28] Therefore, it seems conceivable that catalytic amounts of Sc^{III} ions allow the partial opening/activation of the helical strands and facilitate as well their subsequent exchange with free hydrazines (Figure 8, top). To obtain information about these mechanistic aspects, we performed the partial ^1H NMR titration of helix **1** with increasing amounts of $Sc(OTf)_3$ between 0 and 0.5 equiv (Figure 8, bottom). The observed changes are in agreement with a partial unfolding at the pyridine termini, as indicated by the marked deshielding of the protons located in this *pym*−*hyz*−*pyr* moiety (c−f), while the protons of the central part of the strand are hardly affected (a and b). Moreover, the fact that **11** and **3** are the first two products to be formed, as a function of time, appearing during the equilibration described in Figure 5, supports the hypothesis that, not unexpectedly, the helical strands react first by their more accessible extremities and not by their core hydrazone sites.

(31) In all our attempts involving crossover reactions, the use of the metallic salts $Zn(BF_4)_2 \cdot 8H_2O$ or $Sc(OTf)_3$ avoided the degradation of the library constituents, whereas uncatalyzed and, to a larger extent, proton-catalyzed reactions always underwent extensive side reactions.

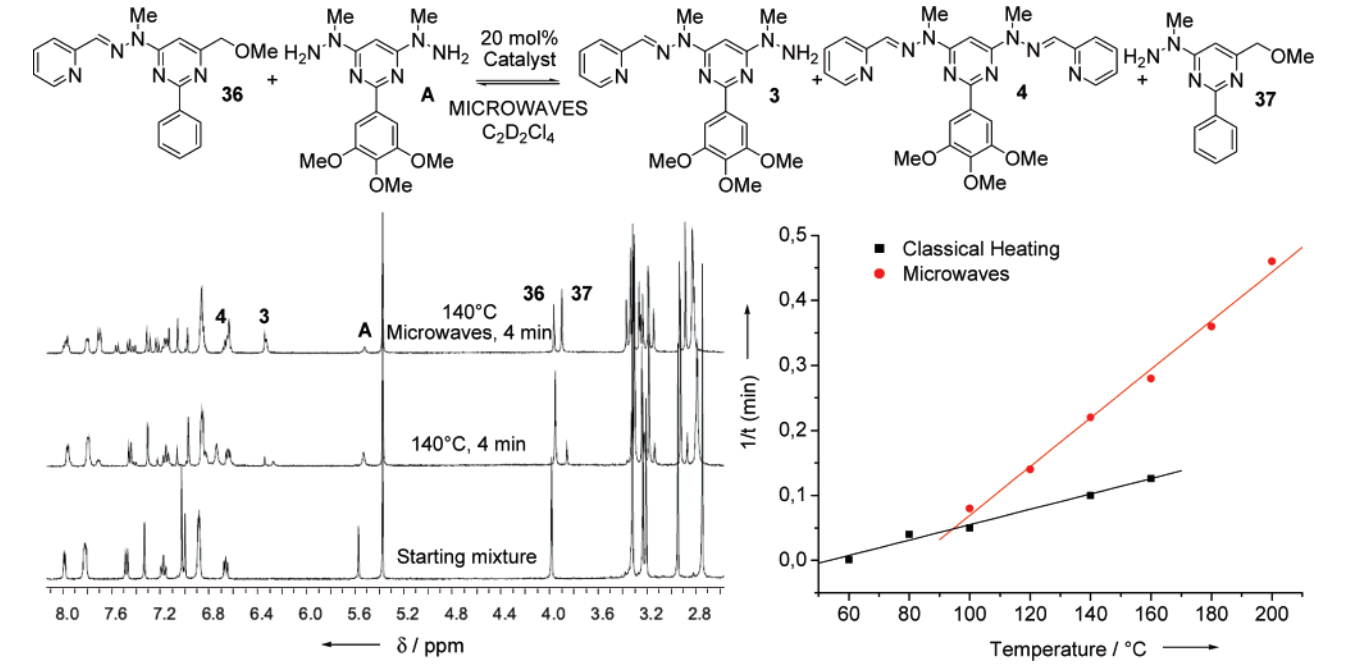

Figure 6. Generation of a model hydrazone/hydrazine equilibrium (top) under Sc^{III} catalysis/microwave activation and followed by ^1H NMR as a function of time and depending on the heating conditions (bottom left); $c(\mathbf{36}) = c(\mathbf{A}) = 5$ mm in $C_2D_2Cl_4$. Comparative catalytic activities of Sc^{III} upon classical/oil bath and microwave heating (bottom right) where t represents the time to reach the equilibrium.

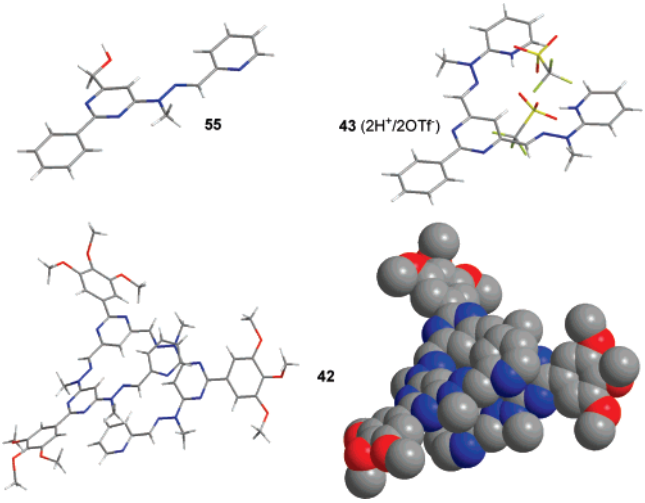

Figure 7. X-ray structures of compounds **55**, bis-protonated **43**, and 1-turn helix **42** (sticks and space-filling representations).

To confirm that the crossover exchange starts at the ends of the strands, nonexchangeable capping-agents were introduced into the helices. To this end, we synthesized both 1-turn (4 sites) and 2-turns (6 sites) helical strands incorporating a non-dynamic terminal pyrimidine−pyridine moiety (single non-reversible connection; "static" capping) at each extremity (type **b** helices **31** and **30**, respectively, Figure 3), as well as their analogues incorporating a pyrimidine−bipyridine moiety, containing two terminal non-reversible connections (type **c** helices **32** (see X-ray in Figure 9) and **29**; "double static" capping). The results of the attempts to perform transimination reactions on these compounds in the presence of bis-hydrazinopyrimidine **A** in the presence of 5 mol % of Sc^{III} catalyst per chelating site are summed in Table 1.

It appears clearly that the presence of nonexchangeable endings "freezes" the constitutional dynamics of the whole strand, despite the presence of exchangeable sites inside the strand. This loss of the exchange and reshuffling capabilities can be directly related to the requirement to partially unfold the strands to activate the first accessible hydrazone site, depending on the nature of the extremities. The unfolding energies have been calculated for the 2-turns helices **17**, **30**, and **29**, respectively (Figure 10), and it was confirmed that this energy increases with the use of more "static" capping moieties. Thus, these observations point to the regioselectivity of the exchange, starting at the termini of the strands due to their folding, and leading to a directional polymerization/depolymerization process. The feasibility of an oriented constitutional elongation/shrinkage process using dissymmetric helices having a single static ending was tested by first synthesizing compound **57**, which can then react with **A** to produce, as a function of time, the various structures described in Figure 11 by reaction at one end only. The reaction was set up in relatively mild conditions (60 °C, [**57**] = 5.7 mm) to keep a slow rate of exchange, which allows the analysis of new crossover products by LC/MS as a function of time. The first set of adducts (**58** and **3**) was observed after a reaction time of 100 min (t_1), the second one (**34**, **6**, **7**, and **4**) after 28 h (t_2), and finally **59** was detected after 60 h (t_3) together with longer strands such as **60** (and others up to 3 turns). These experimental facts, together with the absence at any time of crossover products resulting from the addition of a free hydrazine to an inner hydrazone, agree with the occurrence of an oriented constitutional motional process in this system (see Figure 11, top right).

V. Driven Evolutions of Helical Libraries Toward Metallosupramolecular [2 × 2] Gridlike Arrays. The dynamic library of helical structures under equilibrating conditions, represented in Figure 5, was treated with $Zn(OTf)_2$ (1 equiv with respect to the initial amount of compound **1**). Zn^{II} ions are known to self-assemble with two-site ligands such as **5**, yielding [2 × 2] grid-type complexes in acetonitrile (Figure 12,

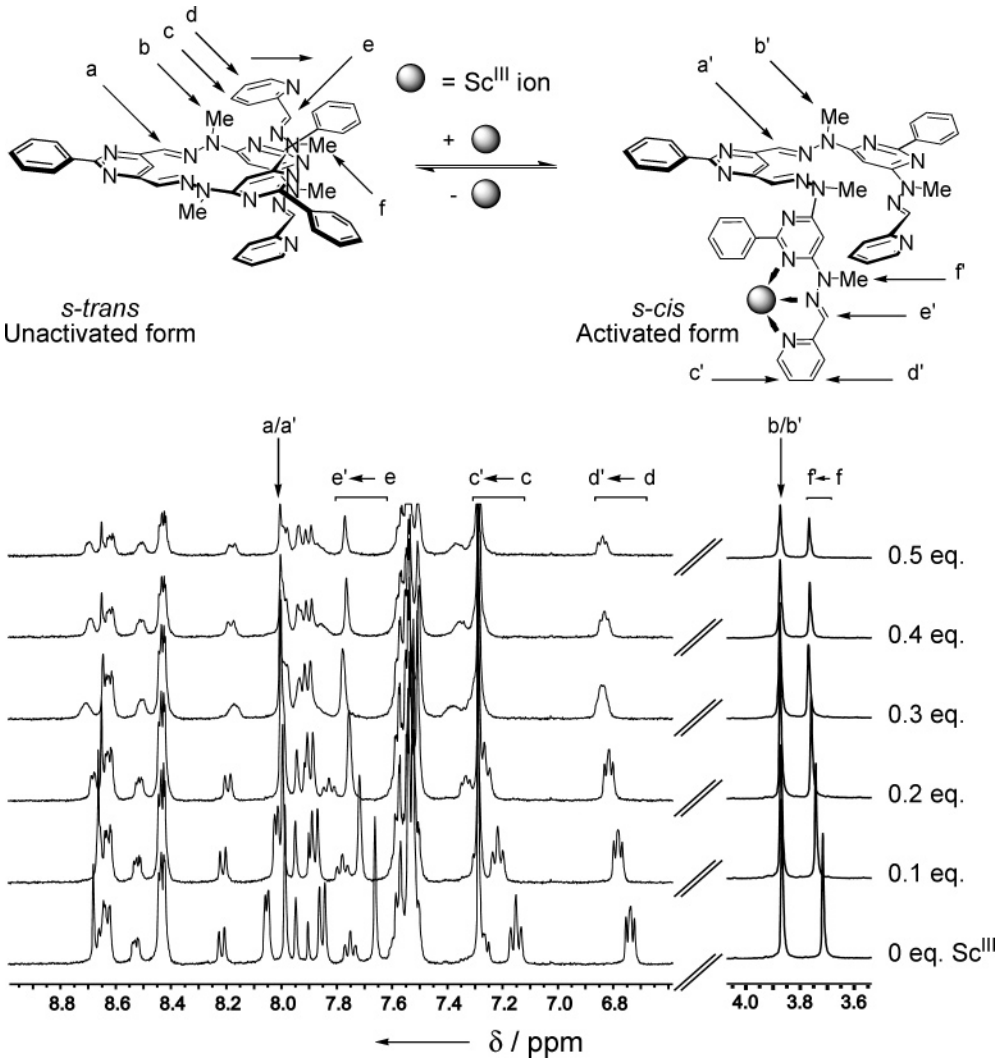

Figure 8. Schematic representation of the partial unfolding of a 1-turn/4-sites *s-trans* helicity-encoded molecular strand upon Sc^{III} chelation and leading to a terminal *s-cis* hydrazone bond, thus activated for transimination reactions (top); selected ^1H NMR spectra of the titration of helical strand **1** (c = 25 mm) by increasing amounts of $Sc(OTf)_3$, between 0 and 0.5 equiv in $CDCl_3$.

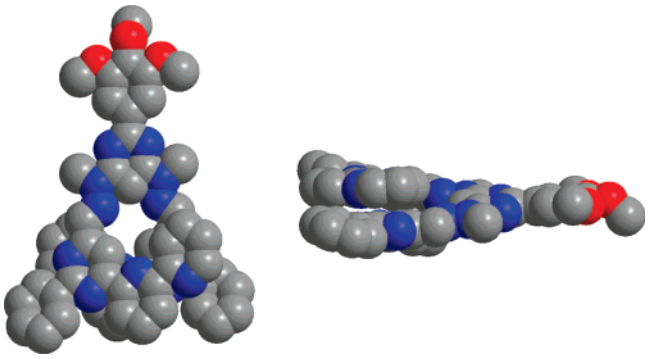

Figure 9. X-ray structure of the 1-turn helical strand **32** containing two non-reversible connections, pyrimidine−pyridine−pyridine (top and side views).

Table 1. Effect of the Presence of Different Capping Agents for the Constitutional Dynamics of the 1-Turn/4-Sites and 2-Turns/6-Sites Helicity-Encoded Molecular Strands upon Sc^{III} Catalysis

crossover reactions with bis-hydrazinopyrimidine **A**[a]	4 sites/1 turn	6 sites/2 turns
type **a** helices ("dynamic" capping)	**1**, exchange	**17**, exchange
type **b** helices ("static" capping)	**31**, exchange	**30**, no exchange
type **c** helices ("double static" capping)	**32**, no exchange	**29**, no exchange

[a] Checked by ^1H NMR and LC/MS after 24 h of heating at 60 °C in $CDCl_3$ in the presence of 5 mol % of $Sc(OTf)_3$ per chelating site.

equilibrium (b)).[32] The formation of $Zn_4\mathbf{5}_4$ as a major tetranuclear grid species, together with the $Zn_4\mathbf{5}_3\mathbf{4}$ and $Zn_4\mathbf{5}_2\mathbf{4}_2$ analogues, was observed by ESI/TOF mass spectroscopy using direct injection. The HPLC trace (b) (displaying the ligands resulting from the dissociation of the complexes on the column) and the ESMS data indicated a marked increase of the amount of **5**, which forms the [2 × 2] grid structure, accompanied by a decrease of the larger helical species, as compared to the initial equilibrium (a). Moreover, Zn^{II} ions favored **5** over **4**, which contains a more bulky central group that hinders the formation of the homoleptic grid complex $Zn_4\mathbf{4}_4$. These observations indicate that the addition of Zn^{II} drives the evolution of the dynamic set toward the expression of ligand **5** under the pressure

(32) Ruben, M.; Lehn, J.-M.; Vaughan, G. *J. Chem. Soc., Chem. Commun.* **2003**, 1338.

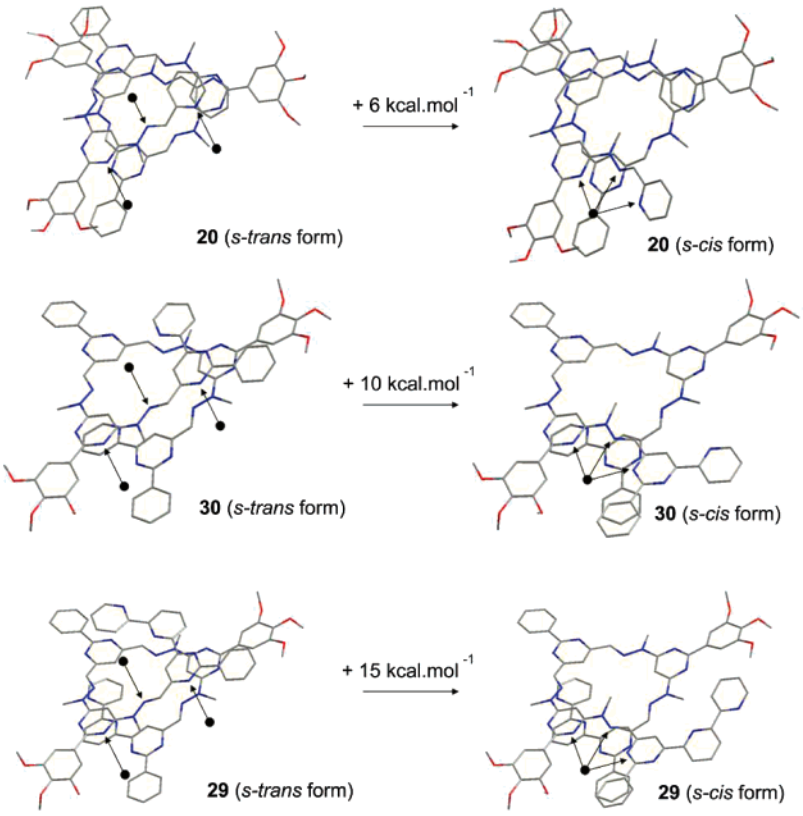

Figure 10. MM2 calculations of the minimum relative energies necessary to allow the constitutional dynamics of the 2-turns/6-sites helicity-encoded molecular strands upon partial unfolding (by a single *s-cis* → *s-trans* conversion) depending on their capping moieties.

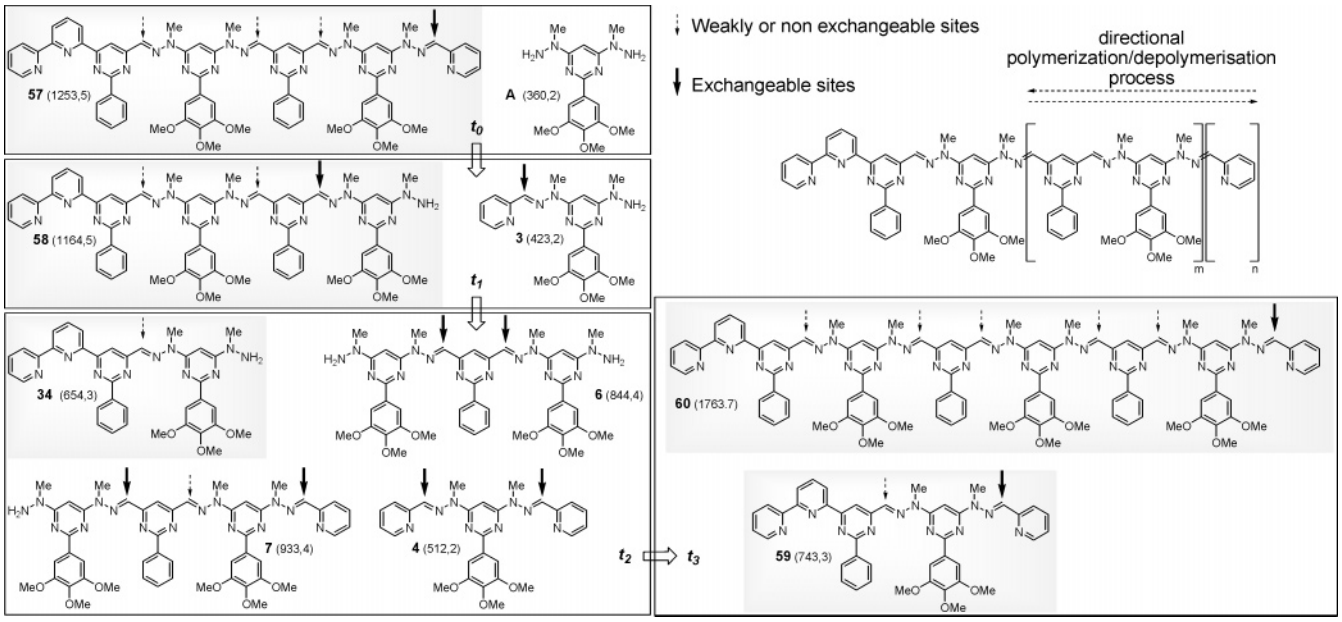

Figure 11. Various structures (and corresponding observed exact masses) obtained by addition of compound **A** on the dissymmetric helical strand **57** (ratio: 1/1) under Sc^{III} catalysis (20 mol %) and as a function of increasing times of reaction (t_0, ..., t_3) : $c_{57} = 5.7$ mm, $T = 60$ °C, $t_0 = 0$, $t_1 = 1$ h 40 min, $t_2 = 28$ h, $t_3 = 60$ h. Each period is the time necessary to generate a new set of compounds, and the drawn structures, until the fourth generation, are limited to the one observed by LC/MS and resulting from the addition of a free hydrazino group to one exchangeable extremity of the library of strands (see dashed and bold plain arrows). (Top right) Schematic directional polymerization/depolymerization process occurring from the reaction of **57** and **A** for the strands bearing the terminal bipyridine unit.[30]

of the formation of the (least bulky) grid-type complex by dissociation and recombination of the subunits of the helical strands to form the corresponding ligand **5**. The process was also found to depend on the Zn^{II} concentration (Figure 10, equilibrium (c)). As shown by the HPLC trace as well as by the direct introduction ESI/TOF mass spectroscopy, when 3 equiv of $Zn(OTf)_2$ was added to the mixture, in addition to an increase of **5** (and of **4** to a lesser extent), the main effect was

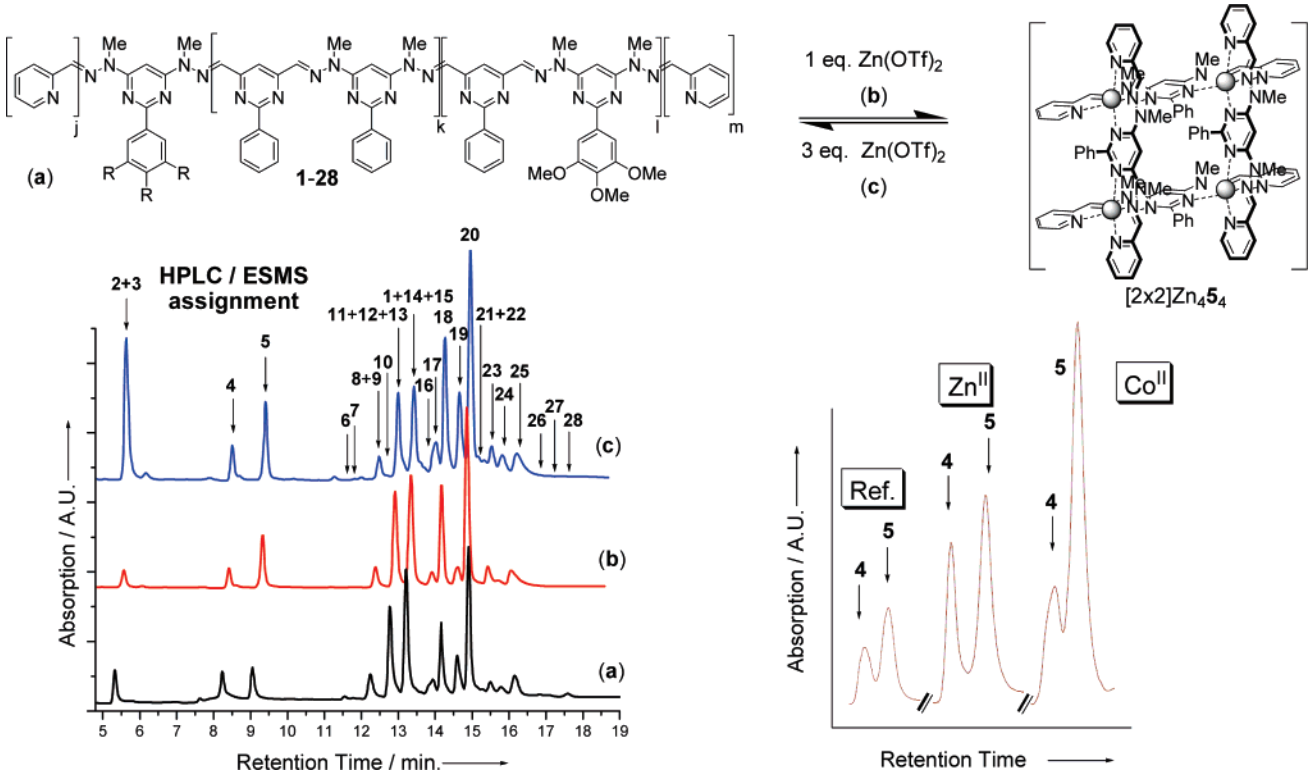

Figure 12. Driven evolution of the dynamic library (a), produced initially from strand **1** (see Figure 5), toward the generation of the [2 × 2] grid complex Zn_4**5**$_4$ (bottom left: HPLC traces) by addition of 1 (b) or 3 (c) equiv of $Zn(OTf)_2$ (CD_3CN; 60 °C; 24 h) to the library (a), pre-equilibrated as in Figure 4 (20% $Sc(OTf)_3$; $CDCl_3$; 60 °C; 48 h), and then evaporated and redissolved in CD_3CN; the equilibrium was not significantly affected by the change in solvent; (bottom right) comparison between the reference (no metal ion), $Zn(OTf)_2$, and $Co(BF4)_2$, for the generation of ligands **4** and **5** as induced by the amplification of the grid-type complex after heating in CD_3CN at 60 °C for 24 h (bottom right: expanded HPLC traces).[30]

the formation of mononuclear Zn**2**$_2$, Zn**23**, and Zn**3**$_2$ complexes, leading to a large amplification of the single site ligands **2** and **3** in the library, as compared to the equilibria (a) and (b). This observation may be accounted for as resulting from the adaptation of the system to generate the ligands providing the sites required for more complete zinc coordination.

We also compared the effect of different metal salts [$Zn(OTf)_2$, $Co(BF4)_2$, $Hg(OAc)_2$, $Pb(OAc)_2$, and $Fe(BF_4)_2$] for the amplification of short ligands through the formation of the corresponding [2 × 2] grids.[8] Whereas Zn^{II} ions led to a light yellow solution, the addition of 1 equiv of Co^{II}, Hg^{II}, Pb^{II}, or Fe^{II} yields light orange, dark red, dark red, and dark green solutions, respectively. The analysis of the HPLC traces showed that Pb^{II}, Hg^{II}, and Fe^{II} gave some supplementary unidentified products, whereas Co^{II} appeared to be the most efficient metal ion for the amplification of **5** (increase by a factor 2 as compared to Zn^{II}, in line with the expected relative stabilities of the grids formed with Zn^{II} and Co^{II} ions) (Figure 12, bottom right).

Next, to set up a system that would be capable of highly selective amplification, we used as starting material the slightly different helical library generated from the 2 sites ligand **43** (Figure 3), in which the positions of the hydrazone sites are reversed as compared to ligand **5**. This connection was chosen as it may be expected to produce in situ, during the library formation, the nucleophilic hydrazinopyridine capping entities **41**, with the correct stoichiometry for converting the set of helices into the ligand necessary for the quantitative formation of the gridlike complex [2 × 2]Zn_4**43**$_4$.

These assumptions were verified experimentally first by ^{1}H NMR studies, as described in Figure 13. Spectrum (a) shows the spectrum, before exchange ($t = 0$), of ligand **43** mixed with 0.5 equiv of bis-hydrazinopyrimidine **A** (to allow generation of a library of helical strands) in the presence of only 10 mol % Sc^{III}. The equilibrium was reached after 18 min upon microwave heating at 140 °C in $CDCl_3$ with the unambiguous formation of a mixture of helical entities, as seen in spectrum b (characteristic triplets below 6.9 ppm). The subsequent treatment of this library with 1 equiv of $Zn(OTf)_2$ in CD_3CN led to a dramatic evolution of the ^{1}H NMR pattern toward spectrum **c**, which is almost superimposable to that of the independently prepared genuine grid complex [2 × 2]Zn_4**43**$_4$ (d). Moreover, the opposite evolution from the grid (d) to the library of helices (b) is also possible by adding 1 equiv of hexamethylhexacyclene to trap Zn^{II} ions and release free **43**.

This spectacular evolution of the library is also confirmed by ESMS spectroscopy (Figure 14). Direct injection of the equilibrated mixture (b in Figure 13) before the addition of Zn^{II} indicates the presence of various helical entities of different sizes, up to 2 turns/6 sites (Figure 14, spectrum a). An almost quantitative shift in the composition of helices via the formation of the grid array is observed in the presence of 1 equiv of $Zn(OTf)_2$ after 3 h at 140 °C (Figure 14, trace c). In the latter spectrum, the assignment of the grid fragments was given by superimposition with the spectrum of the pure [2 × 2]Zn_4**43**$_4$ [see also the HRMS extension of the doubly charged grid [2 × 2]Zn_4**43**$_4(OTf)_6^{2+}$ (e) as well as its theoretical isotopic pattern (f)]. Moreover, spectrum b shows that the grid is kinetically formed from the corner intermediate Zn_2**43**$_2(OTf)_3^+$, which was the major component after 0.5 h (see extension of spectrum d

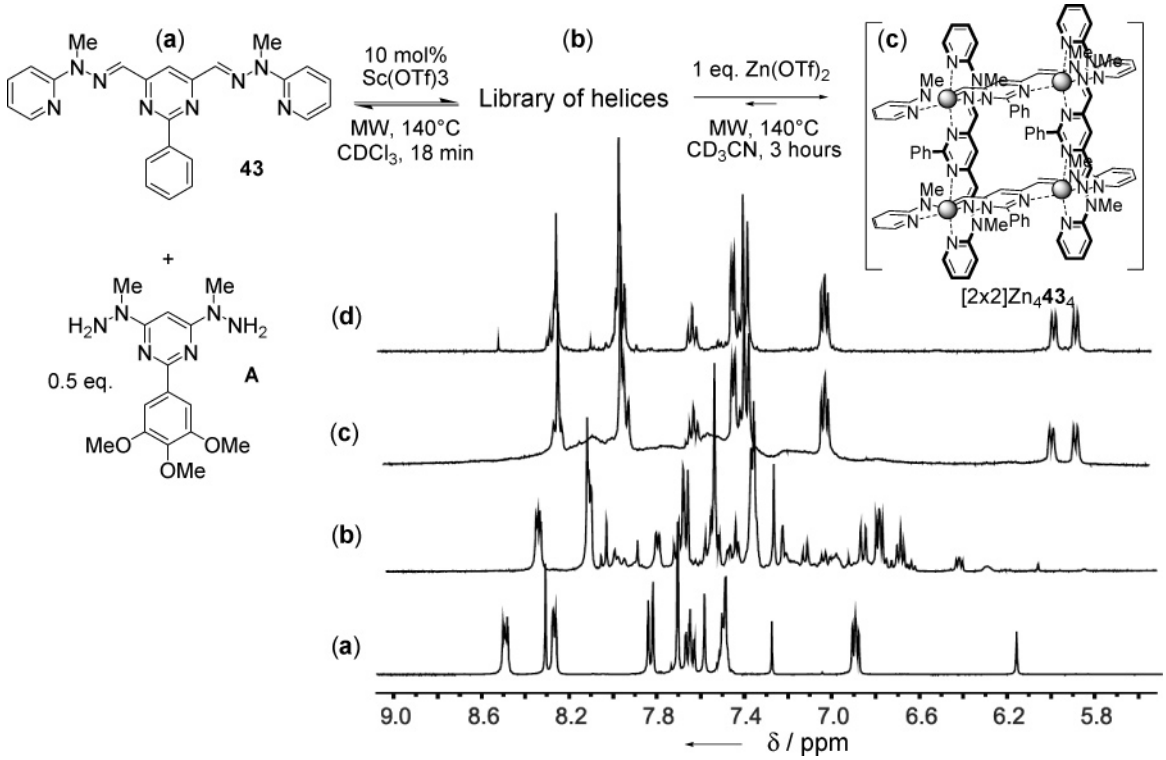

Figure 13. Generation of a library of helicity-encoded molecular strands from the 2-sites compound **43** and bis-hydrazinopyrimidine **A** (0.5 equiv) upon Sc^{III} (10 mol %) catalysis (top left). Subsequent driven evolution of the dynamic library toward the formation of the [2 × 2] grid complex $Zn_4\mathbf{43}_4$ (top right). Bottom right: ^{1}H NMR spectra of the initial mixture **43** + **A** (a), of the equilibrated library of helices after 18 min (b), of the equilibrated library after 3 h in presence of Zn(II) ions (c), and of the separately prepared grid [2 × 2]$Zn_4\mathbf{43}_4$ as reference (d).

showing the mono-charged corner together with some emerging doubly charged grid).

Conclusion

The data reported here provide a general and efficient procedure for the generation of dynamic libraries of constituents, discrete molecules of helical shapes, undergoing assembly, dissociation, and exchange processes, induced by Sc^{III} catalysis and facilitated by microwave activation. The transimination-type mechanism of the Sc^{III}-promoted exchange, as well as its regioselectivity, occurring at the extremities of the strands, allow one to perform directional terminal polymerization/depolymerization processes. These libraries can subsequently be driven by interaction with metal ions (such as Zn^{II} and Co^{II}) toward the amplification of specific ligand constituents, under the pressure of the formation of stable [2 × 2] gridlike coordination architectures (Figure 1). Furthermore, suitable design of these libraries in terms of chemical structures and stoichiometry enables one to make this evolution from helices to grids quantitative. In a broader perspective, the results illustrate the ability of constitutional dynamic systems to respond to environmental parameters and to perform internally (folding) and externally (metal ions) driven evolution toward the fittest constituent, an essential feature characterizing the adaptive and evolutive nature of CDC under the pressure of environmental factors.

Experimental Section

General Aspects. All reagents and solvents were purchased at the highest commercial quality and used without further purification unless otherwise noted. Deuterated chloroform used for the kinetic measurements was flashed through basic alumina immediately prior to use, to remove any trace of acid. Yields refer to purified spectroscopically (^{1}H NMR) homogeneous materials. Thin layer chromatographies were performed with TLC silica plastic sheets (Polygram SIL G/UV_{254}, Macherey-Nagel) or TLC alox plastic sheets (Polygram Alox N/UV_{254}, Macherey-Nagel). In most cases, irradiation using a Bioblock VL-4C UV-lamp (6 W, 254 nm and/or 365 nm) and *p*-anisaldehyde staining were used for visualization. Preparative adsorption flash column chromatographies were performed using silica gel (Geduran, silica gel 60 (230−400 mesh, 40−63 μm, Merck)) and aluminum oxide 90 (Merck; 70−230 mesh, standardized activity II). High-pressure liquid chromatography (HPLC) was carried out on a Hewlett-Packard HP 1100 apparatus equipped with a diode array detector, using a reverse phase column (Thermo, hypersil C_8, 5 cm × 4.6 mm 5 μm). ^{1}H NMR spectra were recorded on a Bruker Avance 400 spectrometer at 400 MHz and ^{13}C spectra at 100 MHz in $CDCl_3$ unless stated otherwise. The spectra were internally referenced to the residual proton solvent signal. In the ^{1}H NMR assignments, the chemical shifts are given in ppm. The coupling constants *J* are listed in Hz. The following notation is used for the ^{1}H NMR spectral splitting patterns: singlet (s), doublet (d), triplet (t), multiplet (m), large (l). The temperatures that are given for the kinetic and thermodynamic data were directly measured and regulated in the NMR probe using a thermocouple. Electrospray (ESI-TOF) studies were performed on a Bruker MicroTOF mass spectrometer (sample solutions were introduced into the mass spectrometer source with a syringe pump with a flow rate of 40 μL min^{-1}). Melting points (Mp) were recorded on a Kofler Heizblock and on a Büchi Melting Point B-540 apparatus and are uncorrected. Microanalyses were performed by the Service de Microanalyse, Institut de Chimie, Université Louis Pasteur. X-ray crystallography: The crystals were placed in oil, and a single crystal was selected, mounted on a glass fiber, and placed in a low-temperature N_2 stream. The X-ray diffraction data were collected on a Nonius-Kappa-CCD diffractometer with graphite monochromatized Mo K_α radiation ($\lambda = 0.71071$ Å), ϕ scans, using a "ϕ scan" type scan mode. The structures were solved using

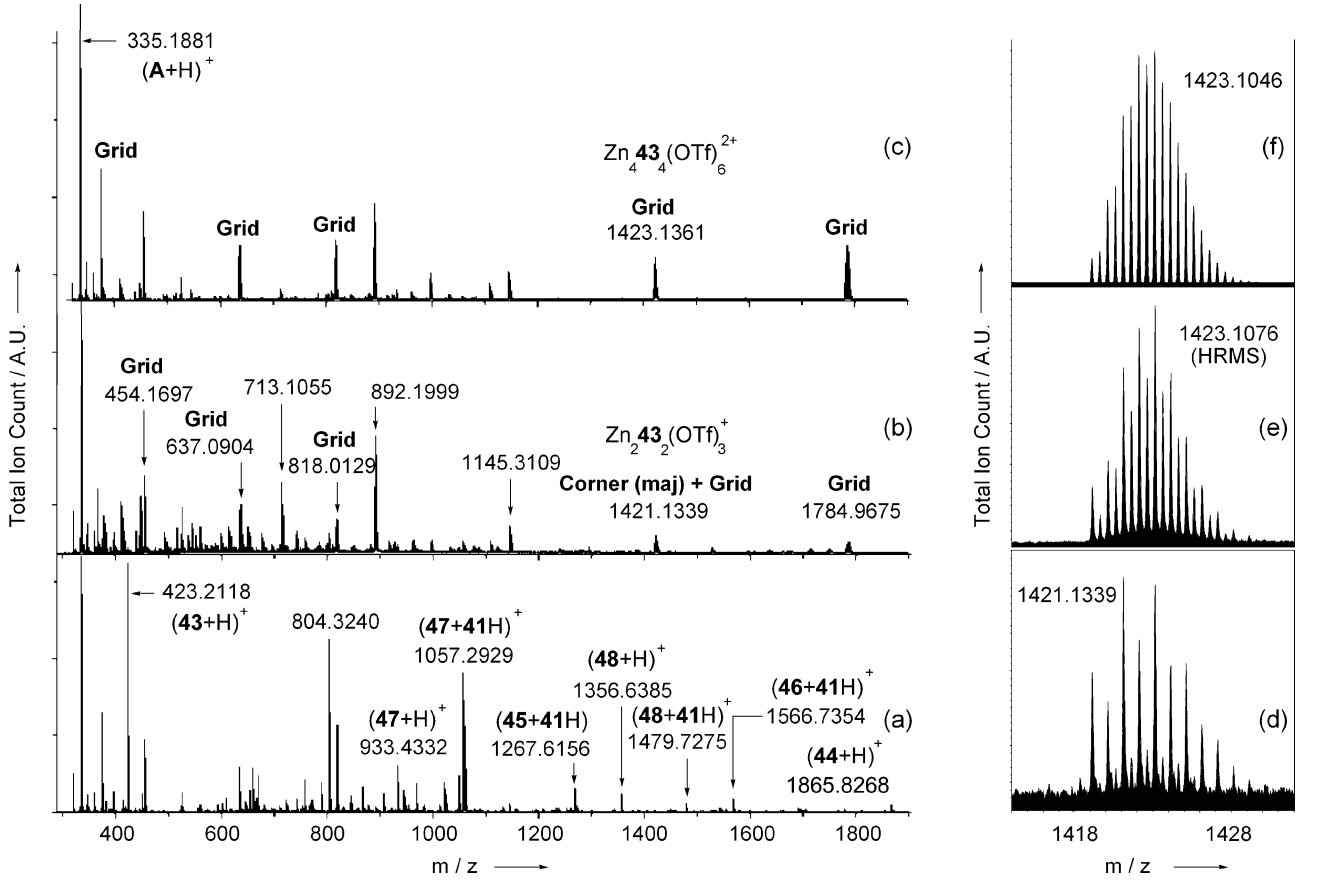

Figure 14. Driven evolution of the dynamic library derived from **43** and **A** (Figure 13, top) toward the generation of the [2 × 2] grid complex Zn_4**43**$_4$. ESMS direct injection spectra: (a) of the library of the molecular strands after 20 min under microwave activation at 140 °C (some products are ionized with protonated compound **41**); (b) of the equilibrated library after 0.5 h at 140 °C in the presence of Zn(II) ions; (c) of the equilibrated library after 3 h at 140 °C in the presence of Zn(II) ions; (d) and (e) are the expansions of the corresponding sets of peaks in spectra b and c, respectively; spectrum f is the calculated isotopic pattern of the grid [2 × 2] Zn_4**43**$_4(OTf)_6^{2+}$. Spectra a−c were obtained using the same spectroscopic/ionization conditions and are directly comparable in terms of intensities.

direct methods and refined (based on F^2 using all independent data) by full-matrix least-squares methods (OpenMolen Package). CCDC 620827−620830 contain the supplementary crystallographic data for this paper. These data can be obtained free of charge from the Cambridge Crystallographic Data Center via www.ccdc.ac.uk/data_request/cif. All molecular representations (Stick, CPK) and 3D-images in this Article were created using WebLabViewer Pro (ver. 5, 2002, Accelrys). Microwave heating was performed using a CEM discover with closed vessels filled with 1−2 mL solutions. The regulation of the heating was done by fixing the temperature and without regulation of the power or the pressure. LC/MS was performed by coupling a Hewlett-Packard HP 1100 chromatography apparatus and either a Thermo Finnigan Surveyor MSQ mass spectrometer or a Bruker MicroTOF mass spectrometer. The samples were prepared from an aliquot of the mixtures under equilibration, diluted 1000 times in a solution of $CHCl_3$/MeOH (2/3:1/3).

General Procedure for Crossover Experiments and Determinations of Kinetic Data. A typical protocol is realized by the preparation of a fresh $CDCl_3$ solution containing the compounds to exchange in a NMR tube (0.6 mL, 22.6 mM in hydrazone) or a vial (2 mL, 22.6 mM in hydrazone). The desired amounts of catalyst were immediately added to this mixture from a CD_3CN solution (5−50 μL, 45 mM, 0.2−8.0 vol % of CD_3CN in $CDCl_3$), prior to NMR measurements. The first spectrum was usually recorded 30 s after addition without spinning in the probe. The NMR tubes were topped with Teflon caps to keep a constant concentration upon heating.

Procedure for the Driven Evolutions of Helical Libraries Toward Metallosupramolecular [2 × 2] Gridlike Arrays (Examples of Figures 13 and 14). Compound **43** (21.15 mg, 5×10^{-3} mmol) and bis-hydrazinopyrimidine **A** (8.3 mg, 2.5×10^{-3} mmol) were dissolved in 2 mL of $CDCl_3$. The catalyst (10%) was added via a microsyringe (15 μL) from of a solution of $Sc(OTf)_3$ in CD_3CN (90 mg in 0.5 mL). The yellow solution was heated in a closed vial adapted to the microwave apparatus at 140 °C for 18 min. Next, the solvent was evaporated to almost dryness under reduced pressure, and the residue was dissolved using a solution of $Zn(OTf)_2$ (18 mg, 5×10^{-3} mmol) in 1 mL of CD_3CN. After 3 h of heating under microwaves at 140 °C, the solution turned dark red/brown, the characteristic color of grid [2 × 2]Zn_4**43**$_4$.

Procedures for the Syntheses and Characterizations of the Products. Products **A**, **B**, **1**, **2**, **4**−**6**, **20**, **41**, **43** are described in ref 12b, products **39** and **40** are in ref 12a, and grids [2 × 2]Zn_4**5**$_4$ and [2 × 2]Zn_4**43**$_4$ are described in ref 33.

Pyridine-2-carboxaldehyde Methyl[6-(1-methylhydrazino)-2-(3,4,5-trimethoxyphenyl)pyrimidin-4-yl]hydrazone (3). To a solution of 4,6-bis(*N*-methylhydrazino)-2-(3,4,5-trimethoxyphenyl)pyrimidine **A**[12b] (250 mg, 74×10^{-2} mmol) in a mixture of absolute ethanol (20 mL) and $CHCl_3$ (13 mL) was added a solution of pyridine-2-carboxaldehyde (80 mg, 74×10^{-2} mmol) in 20 mL of absolute ethanol. The solution was stirred at room temperature for 24 h under an atmosphere of argon. All of the solvents were then removed under reduced pressure, and the residue was purified by flash chromatography (Al_2O_3, AcOEt/Hex, 1/1) to give **3** (170 mg, 51%) as a white solid.

(33) Barboiu, M.; Ruben, M.; Blasen, G.; Kyritsakas, N.; Chacko, E.; Dutta, M.; Radekovich, O.; Lenton, K.; Brook, D. J. R.; Lehn, J.-M. *Eur. J. Inorg. Chem.* **2006**, 784.

Mp 162−165 °C. ^{1}H NMR: 8.57 (d, ^3J = 4.8 Hz, 2H), 8.0 2 (d, ^3J = 5.4 Hz, 2H), 7.54 (s, 1H), 7.73 (m, 3H), 7.21 (t, ^3J = 5.4 Hz, 1H), 6.95 (s, 1H), 3.96 (s, 6H), 3.90 (s, 3H), 3.77 (s, 3H), 3.42 (s, 3H). ^{13}C NMR: 163.1, 155.1, 153.0, 149.3, 140.3, 137.0, 136.6, 136.4, 136.1, 122.9, 119.9, 105.3, 86.8, 60.9, 56.1, 29.8, 29.7. HRMS (ESi-TOF-MS) *m*/*z* (%): calcd for $C_{21}H_{25}N_7O_3$ 446.1916 $[M + H]^+$; found 446.1750 (100) $[M + Na]^+$.

2-Phenylpyrimidine-4,6-dicarboxaldehyde 4,4-Bis{methyl{6-[1-methyl-2-(pyridin-2-ylmethylene)hydrazino]-2-(3,4,5-trimethoxyphenyl)pyrimidin-4-yl}hydrazone} 6,6-{[2-(3,4,5-Trimethoxyphenyl)pyrimidine-4,6-diyl]bis(methylhydrazone)} (17). To a solution of 4,6-bis(*N*-methylhydrazino)-2-(3,4,5-trimethoxyphenyl)pyrimidine **A**[12b] (5 mg, 1.49 × 10^{-2} mmol) in a $CHCl_3$ solution (0.8 mL) was added **35** (18.5 mg, 2.99 × 10^{-2} mmol). The solution was stirred at 60 °C overnight under an atmosphere of argon. All of the solvent was then removed under reduced pressure, and the residue was purified by flash chromatography (silica gel, gradient of solvents: $CHCl_3$ to $CHCl_3$/MeOH (95/5)) to give **17** (22 mg, 96%) as a yellow powder. Mp > 250 °C (decomposition). ^{1}H NMR: 8.39 (s, 2H), 8.20 (dd, ^3J = 8.6 Hz, ^3J = 1.2 Hz, 4H), 8.03 (d, ^3J = 4.3 Hz, 2H), 7.69 (d, ^3J = 7.8 Hz, 2H), 7.64 (d, ^3J = 5.8 Hz, 4H), 7.60 (s, 2H), 7.57 (s, 2H), 7.45 (s, 4H), 7.42 (s, 2H), 7.35 (t, ^3J = 7.4 Hz, 2H), 7.22 (t, ^3J = 7.0 Hz, 4H), 7.22 (s, 1H), 6.98 (t, ^3J = 7.4 Hz, 2H), 6.64 (dd, ^3J = 6.2 Hz, ^3J = 1.2 Hz, 2H), 4.10 (s, 6H), 4.02 (s, 3H), 4.00 (s, 6H), 3.89 (s, 12H), 3.80 (s, 6H), 3.68 (s, 12H).^{13}C NMR: 164.45, 162.45, 162.00, 161.45, 161.30, 161.20, 161.05, 160.75, 153.75, 153.05, 152.60, 140.30, 140.05, 137.05, 135.50, 135.25, 135.15, 133.50, 133.10, 130.30, 127.95, 127.90, 122.00, 119.30, 106.95, 105.40, 105.15, 89.00, 87.30, 61.00, 60.85, 56.30, 55.95, 30.15, 30.05, 29.80. HRMS (ESi-TOF-MS) *m*/*z* (%): calcd for $C_{81}H_{81}N_{24}O_9$ 1533.6618 $[M + H]^+$; found 1533.6625 (100) $[M + H]^+$.

(1*E*,1′*E*)-(2,2′-(6,6′-(2*E*,2′*E*)-2,2′-(2-Phenylpyrimidine-4,6-diyl)bis(methan-1-yl-1-ylidene)bis(1-methylhydrazin-1-yl-2-ylidene)bis(2-(3,4,5-trimethoxyphenyl)pyrimidine-6,4-diyl))bis(2-methylhydrazin-2-yl-1-ylidene))bis(methan-1-yl-1-ylidene)bis(2-phenylpyrimidine-6,4-diyl))di-2,2′-bipyridine (29). 6-(2,2′-Bipyridin-6-yl)-2-phenylpyrimidine-4-carbaldehyde **53** (30 mg, 8.9 × 10^{-2} mmol) and 4,6-bis(1-methylhydrazinyl)-2-(3,4,5-trimethoxyphenyl)pyrimidine (30 mg, 0.089 mmol) were stirred in 2 mL of chloroform at 40 °C for 2 h under an atmosphere of argon. 4,6-Diformyl-2-phenyl-pyrimidine (9.5 mg, 0.045 mmol) was then added and stirred at 40 °C for 12 h. After the solvent was removed under reduced pressure, the residue was purified by chromatography (Al_2O_3, $CHCl_3$) to give **29** (15 mg, 23%) as a yellow solid. Mp > 250 °C (decomposition). ^{1}H NMR: 8.88 (s, 1H), 8,57 (d, ^3J = 8.0 Hz, 2H), 8.40 (d, ^3J = 7.2 Hz, 2H), 8.31 (d, ^3J = 7.2 Hz, 4H), 8.08 (m, 5H), 7.97 (t, ^3J = 8.0 Hz, 2H), 7.74 (s, 2H), 7.54 (d, ^3J = 6 Hz, 4H), 7.50 (s, 2H), 7.45 (s, 4H), 7.26 (m, 4H), 7.23 (t, ^3J = 8 Hz, 2H), 7.05 (s, 2H), 6.85 (s, 2H), 6.71 (m, 2H), 4.01 (s, 6H), 3.93 (s, 12H), 3.82 (s, 6H), 3.42 (s, 6H). ^{13}C NMR: 164.04, 162.62, 162.49, 162.33, 161.348, 160.75, 155.693, 154.86, 153.83, 152.96, 148.62, 140.50, 138.41, 137.60, 137.41, 135.96, 135.62, 133.44, 130.59, 128.91, 128.62, 128.29, 123.67, 122.47, 121.39, 120.91, 109.44, 105.57, 87.65, 61.20, 56.34, 34.24, 32.24. HRMS (ESi-TOF-MS) *m*/*z* (%): calcd for $C_{84}H_{73}N_{22}O_6$ 1485.6078 $[M + H]^+$; found 1485.6279 (100) $[M + H]^+$.

(1*E*,1′*E*)-(2,2′-(6,6′-(2*E*,2′*E*)-2,2′-(2-Phenylpyrimidine-4,6-diyl)bis(methan-1-yl-1-ylidene)bis(1-methylhydrazin-1-yl-2-ylidene)bis(2-(3,4,5-trimethoxyphenyl)pyrimidine-6,4-diyl))bis(2-methylhydrazin-2-yl-1-ylidene))bis(methan-1-yl-1-ylidene)bis(2-phenylpyrimidine-6,4-diyl))di-2,2′-pyridine (30). A solution of **33** (30.8 mg, 4.7 × 10^{-2} mmol) and 2-phenylpyrimidine-4,6-dicarboxaldehyde[12b] (5 mg, 2.35 × 10^{-2} mmol) in 1.2 mL of $CHCl_3$ was stirred at room temperature for 12 h under an argon atmosphere. Chloroform was then removed under reduced pressure, and the residue was purified by flash chromatography (silica gel, $CHCl_3$) to afford **30** (30 mg, 96%) as a pale yellow powder. Mp > 250 °C (decomposition). ^{1}H NMR: 8.75 (l, 2H), 8.55 (d, ^3J = 7.8 Hz, 4H), 8.47 (s, 1H), 8.29 (d, ^3J = 7.4 Hz, 4H), 7.96 (l, 2H), 7.86 (t, ^3J = 6.4 Hz, 2H), 7.65 (s, 2H), 7.64−7.50 (m, 3H), 7.56 (s, 2H), 7.43 (s, 4H), 7.32 (t, ^3J = 6.8 Hz, 4H), 7.20 (t, ^3J = 6.8 Hz, 4H), 7.17−7.15 (m, 2H), 7.14 (s, 2H), 4.01 (s, 6H), 3.92 (s, 12H), 3.79 (s, 6H), 3.39 (s, 6H). ^{13}C NMR: 164.25, 163.70, 162.10, 161.90, 161.85, 160.85, 154.35, 152.55, 149.00, 139.95, 138.10, 137.15, 136.25, 134.95, 133.10, 130.55, 130.20, 128.65, 128.15, 127.90, 127.80, 124.80, 120.95, 105.10, 88.20, 60.85, 55.95, 30.10, 29.25. HRMS (ESi-TOF-MS) *m*/*z* (%): calcd for $C_{74}H_{67}N_{20}O_6$ 1331.5547 $[M + H]^+$; found 1331.5512 (100) $[M + H]^+$.

6,6′-(6,6′-(1*E*,1′*E*)-(2,2′-(2-(3,4,5-Trimethoxyphenyl)pyrimidine-4,6-diyl)bis(2-methylhydrazin-2-yl-1-ylidene))bis(methan-1-yl-1-ylidene)bis(2-phenylpyrimidine-6,4-diyl))di-2,2′-pyridine (31). To a solution of 2-phenyl-6-(pyridin-2-yl)pyrimidine-4-carbaldehyde **54** (94 mg, 2.77 × 10^{-1} mmol) in $CHCl_3$ (2 mL) was added 4,6-bis(*N*-methylhydrazino)-2-(3,4,5-trimethoxyphenyl)pyrimidine **A**[12b] (46.4 mg, 1.38 × 10^{-1} mmol). The solution was stirred at room temperature overnight under an atmosphere of argon. All of the solvent was then removed under reduced pressure, and the residue was purified by flash chromatography (silica gel, $CHCl_3$) to give a mixture of **31** (top spot, 62 mg, 55%, yellow powder) and of the corresponding monohydrazine **33** (bottom spot, 38 mg, yellow powder). **31**, Mp > 250 °C (decomposition). ^{1}H NMR: 8.95 (s, 2H), 8.73−8.63 (m, 4H), 8.22 (s, 1H), 8.14 (d, ^3J = 7.9 Hz, 2H), 8.00 (s, 2H), 7.85 (s, 2H), 7.60−7.50 (m, 8H), 7.55 (td, ^3J = 7.6 Hz, ^3J = 1.7 Hz, 2H), 6.96 (ddd, ^3J = 7.3 Hz, ^3J = 4.7 Hz, ^3J = 1.2 Hz, 2H), 4.06 (s, 6H), 3.99 (s, 3H), 3.94 (s, 6H). ^{13}C NMR: 164.00, 163.25, 162.80, 161.95, 153.85, 153.10, 153.00, 148.50, 137.95, 136.05, 135.25, 133.40, 130.60, 128.55, 128.20, 124.55, 120.80, 110.25, 105.45, 101.95, 89.10, 61.00, 56.20, 30.15. HRMS (ESi-TOF-MS) *m*/*z* (%): calcd for $C_{47}H_{41}N_{12}O_3$ $[M + H]^+$ 821.3419; found 821.3453 (100) $[M + H]^+$. **33**, ^{1}H NMR: 8.84 (s, 1H), 8.76 (d, ^3J = 3.9 Hz, 1H), 8.70 (d, ^3J = 8.2 Hz, 1H), 8.64 (m, 2H), 7.92 (td, ^3J = 7.8 Hz, ^3J = 1.6 Hz, 2H), 7.85 (s, 1H), 7.76 (s, 2H), 7.58−7.55 (m, 2H), 7.44 (ddd, ^3J = 7.0 Hz, ^3J = 4.7 Hz, ^3J = 1.2 Hz, 1H), 7.11 (s, 1H), 4.00 (s, 6H), 3.95 (s, 3H), 3.82 (s, 3H), 3.48 (s, 3H). ^{13}C NMR: 165.40, 164.35, 163.25, 162.70, 162.50, 161.75, 154.60, 152.95, 149.40, 140.20, 137.75, 137.10, 134.55, 133.85, 130.65, 128.50, 128.25, 125.20, 121.95, 109.90, 105.35, 83.35, 60.95, 56.15, 39.70, 30.10, 28.25. HRMS (ESi-TOF-MS) *m*/*z* (%): calcd for $C_{31}H_{32}N_9O_3$ 578.2623 $[M + H]^+$; found 578.2625 (100) $[M + H]^+$.

6,6′-(6,6′-(1*E*,1′*E*)-(2,2′-(2-(3,4,5-Trimethoxyphenyl)pyrimidine-4,6-diyl)bis(2-methylhydrazin-2-yl-1-ylidene))bis(methan-1-yl-1-ylidene)bis(2-phenylpyrimidine-6,4-diyl))di-2,2′-bipyridine (32). 6-(2,2′-Bipyridin-6-yl)-2-phenylpyrimidine-4-carbaldehyde **53** (30 mg, 8.9 × 10^{-2} mmol) and 4,6-bis(1-methylhydrazinyl)-2-(3,4,5-trimethoxyphenyl)pyrimidine (14.5 mg, 4.5 × 10^{-2} mmol) were stirred in 2 mL of chloroform at 40 °C for 12 h under an atmosphere of argon. The solvent was then removed under reduced pressure, and the residue was purified by chromatography (Al_2O_3, $CHCl_3$) to give **32** (30 mg, 69%) as a yellow solid. Mp > 250 °C (decomposition). ^{1}H NMR: 8.82 (s, 2H), 8.40 (m, 4H), 8.19 (m, 7H), 8.08 (d, ^3J = 8.2 Hz, 2H), 7.86 (s, 2H), 7.80 (s, 2H), 7.64 (t, ^3J = 8.0 Hz, 2H), 7.55 (m, 6H), 7.36 (td, ^3J = 8.2 Hz, ^3J = 1.2 Hz, 2H), 6.93 (t, ^3J = 5.4 Hz, 2H), 4.09 (s, 6H), 4.01 (s, 3H), 3.90 (s, 6H). ^{13}C NMR: 163.78, 163.30, 162.29, 162.23, 154.72, 154.53, 153.13, 152.80, 148.33, 137.78, 137.21, 136.32, 135.68, 132.91, 132.13, 132.04, 131.95, 130.34, 128.54, 128.42, 128.33, 128.28, 123.42, 121.91, 121.27, 120.28, 109.53, 105.51, 87.22, 60.99, 56.24, 30.25. HRMS (ESi-TOF-MS) *m*/*z* (%): calcd for $C_{57}H_{46}N_{14}Na_1O_3$ 997.3770 $[M + Na]^+$; found 997.3771 (100) $[M + Na]^+$.

Crystal Structure of 32 (CCDC 620830). A suitable crystal of **32** was obtained by diffusion−recrystallization from $CHCl_3$ (solvent). Diffraction data were collected at 173 K. Formula: $C_{60}H_{49}Cl_9N_{14}O_3$ = $C_{57}H_{46}N_{14}O_3$·3$CHCl_3$. Molecular weight: 1333.18. Yellow crystal; crystal size (mm): 0.18 × 0.14 × 0.10. Unit cell parameters: a = 13.8400 (3) Å, b = 15.0840(3) Å, c = 16.3080(4) Å, α = 82.84(5)°, β = 70.59°(5), γ = 75.03(5)°; crystal system, triclinic; space group *P*-1; V = 3099.2(1) Å^3; F(000) = 1368; Z = 2; calculated density = 1.43 g cm^{-3}; linear absorption coefficient μ = 0.464 mm^{-1}. Of 21 844

reflections measured, 14 155 reflections were unique ($I > 3\sigma(I)$); 877 refined variables. The θ range for data collection was 1.33−27.50° with *hkl* limits: −19 to 19, −19 to 21, and −19 to 22. The final indices were $R = 0.0866$ and $R_w = 0.2108$, with a goodness-of-fit (GOF) of 1.031. The largest peak in final difference was 0.831 e Å^{-3}.

(*E*)-6-(6-((2-Methyl-2-(6-(1-methylhydrazinyl)-2-(3,4,5-trimethoxyphenyl)pyrimidin-4-yl)hydrazono)methyl)-2-phenylpyrimidin-4-yl)-2,2′-bipyridine (34). 6-(2,2′-Bipyridin-6-yl)-2-phenylpyrimidine-4-carbaldehyde **53** (30 mg, 8.9 × 10^{-2} mmol) and 4,6-bis(1-methylhydrazinyl)-2-(3,4,5-trimethoxyphenyl)pyrimidine (29 mg, 9 × 10^{-2} mmol) were stirred in 2 mL of chloroform at 40 °C for 12 h under an atmosphere of argon. The solvent was then removed under reduced pressure, and the residue was purified by chromatography (Al_2O_3, $CHCl_3$) to give **34** (30 mg, 50%) as a yellow solid. ^{1}H NMR: 8.99 (s, 1H), 8.78 (m, 2H), 8.68 (m, 3H), 8.60 (d, ^3J = 6.8 Hz, 1H), 8.08 (t, ^3J = 8.0 Hz, 1H), 7.96 (s, 1H), 7.88 (t, ^3J = 8.0 Hz, 1H), 7.79 (s, 2H), 7.57 (m, 3H), 7.36 (t, ^3J = 8.0 Hz, 1H), 7.15 (s, 1H), 4.03 (s, 6H), 3.96 (s, 3H), 3.91 (s, 3H). ^{13}C NMR: 165.37, 164.20, 162.95, 162.41, 161.74, 157.04, 156.01, 155.63, 153.95, 152.96, 149.30, 137.90, 136.57, 135.17, 130.69, 128.51, 128.27, 123.84, 122.65, 122.03, 120.76, 105.40, 83.14, 79.17, 60.93, 56.17, 39.96, 39.85, 29.70. HRMS (ESi-TOF-MS) *m*/*z* (%): calcd for $C_{36}H_{35}N_{10}O_3$ 655.2888 [M + H]$^+$; found 655.2977 (100) [M + H]$^+$.

2-Phenylpyrimidine-4,6-dicarboxaldehyde Mono{methyl{6-[1-methyl-2-(pyridin-2-ylmethylene)hydrazino]-2-(3,4,5-trimethoxyphenyl)pyrimidin-4-yl}hydrazone} (35). A solution of **3** (120 mg, 0.28 mmol) and 2-phenylpyrimidine-4,6-dicarboxaldehyde[12c] (56 mg, 0.28 mmol) in 25 mL of CH_2Cl_2 was stirred at room temperature for 2 h under an argon atmosphere. The reaction mixture was then cooled to 0 °C and filtered to give **35** as a yellow powder (104 mg, 60%). Mp 249 °C. ^{1}H NMR: 10.22 (s, 1H), 8.66 (d, ^3J = 4.4 Hz, 2H), 8.61 (m, 2H), 8.39 (s, 1H), 8.34 (d, ^3J = 8.0 Hz, 1H), 8.20 (t, ^3J = 8.0 Hz, 1H), 8.01 (s, 1H), 7.92 (s, 1H), 7.80 (m, 4H), 7.58 (m, 4H), 7.32 (t, ^3J = 8.0 Hz, 1H), 4.02 (s, 6H), 3.98 (s, 3H), 3.91 (s, 3H), 3.86 (s, 3H). ^{13}C NMR: 193.4, 165.8, 164.2, 163.4, 162.7, 161.8, 158.3, 154.4, 153.2, 149.2, 138.9, 137.6, 136.7, 134.5, 133.26, 131.3, 128.6, 123.3, 119.8, 87.2, 60.8, 56.2, 30.4, 29.9. Anal. Calcd for $C_{33}H_{31}N_9O_4$: C, 64.17; H, 5.06; N, 20.41. Found: C, 63.54; H, 4.99; N, 19.98. ESI-TOF-MS *m*/*z* (%): 618.2 (100) [M + H]$^+$.

1-(6-(Methoxymethyl)-2-phenylpyrimidin-4-yl)-1-methyl-2-(pyridin-2-ylmethylene)hydrazine (36). A solution of **37** (0.3 mg, 1.23 mmol) and pyridine-2-carboxaldehyde (133 mg, 1.23 mmol) in 8 mL of absolute ethanol was stirred at room temperature for 4 h under an argon atmosphere. The solution was then concentrated under reduced pressure and filtered to give **36** (333 mg, 81%) as a white solid. Mp 134−136 °C. ^{1}H NMR: 8.55 (d, ^3J = 4.8 Hz, 1H), 8.44 (m, 2H), 8.10 (d, ^3J = 8.0 Hz, 1H), 7.93 (s, 1H), 7.77 (t, ^3J = 8.0 Hz, 1H), 7.65 (s, 1H), 7.47 (m, 3H), 7.26 (t, ^3J = 8.0 Hz, 1H), 4.60 (s, 2H), 3.83 (s, 3H), 3.57 (s, 3H). ^{13}C NMR: 166.7, 163.1, 163.0, 154.5, 149.3, 138.3, 137.9, 136.5, 130.4, 128.3, 127.1, 123.27, 119.8, 100.6, 74.9, 59.0, 29.4. Anal. Calcd for $C_{19}H_{19}N_5O$: C, 68.45; H, 5.74; N, 21.01. Found: C, 68.41; H, 6.14; N, 20.60. ESI-TOF-MS *m*/*z* (%): 334.2 (100) [M + H]$^+$.

1-(6-(Methoxymethyl)-2-phenylpyrimidin-4-yl)-1-methylhydrazine (37). Methylhydrazine (0.3 mL, 5.64 mmol) was added to a solution of 4-chloro-6-methoxymethyl-2-phenylpyrimidine **39**[12a] (0.5 g, 2.15 mmol) in ethanol (6 mL). The mixture was then heated to reflux for 48 h under an atmosphere of argon. Upon subsequent cooling to 0 °C, crystallization occurred. The crystals were filtered, washed with ethanol, and air-dried to afford **37** (0.42 g, 80%) as a white powder. Mp 101−102 °C. ^{1}H NMR: 8.39 (m, 2H), 7.43 (m, 3H), 6.87 (s, 1H), 4.52 (s, 2H), 3.52 (s, 3H), 3.42 (s, 3H). ^{13}C NMR: 165.7, 163.2, 138.4, 130.1, 128.2, 128.1, 97.14, 93.4, 74.9, 58.9, 39.6. ESI-TOF-MS *m*/*z* (%): 245.1 (100) [M + H]$^+$. Anal. Calcd for $C_{13}H_{16}N_4O$: C, 63.91; H, 6.60; N, 22.93. Found: C, 63.58; H, 6.62; N, 23.13.

(6-(1-Methylhydrazino)-2-phenylpyrimidin-4-yl)methanol (38). To a solution of (6-chloro-2-phenylpyrimidin-4-yl)methanol **40**[12a] (3.6 g, 16.3 mmol) in ethanol (50 mL) was added methylhydrazine (3 mL, 56.4 mmol). The mixture was then heated to reflux for 48 h under an argon atmosphere. Upon subsequent cooling to 0 °C, crystallization occurred. The crystals were filtered, washed with ethanol, and air-dried to afford **38** as a white powder (2.8 g, 74%). Mp 137−138 °C. ^{1}H NMR (DMSO-d_6): 8.34 (m, 2H), 7.45 (m, 3H), 5.38 (s, 1H), 4.83 (s, 2H), 4.45 (d, 2H), 3.39 (s, 3H). ^{13}C NMR (DMSO-d_6): 169.9, 165.3, 161.7, 138.7, 130.3, 128.6, 128.0, 97.75, 64.2, 39.4. Anal. Calcd for $C_{12}H_{14}N_4O$: C, 62.59; H, 6.13; N, 24.33. Found: C, 62.63; H, 5.89; N, 24.44. ESI-TOF-MS *m*/*z* (%): 231.1 (100) [M + H]$^+$.

2-Phenylpyrimidine-4,6-dicarboxaldehyde Mono{methyl{6-[1-methyl-2-(pyridin-2-ylmethylene)hydrazino]-2-phenylpyrimidin-4-yl}hydrazone} (42). A solution of **3** (10 mg, 2.6 × 10^{-2} mmol) and 4,6-diformyl-2-(3,4,5-trimethoxyphenyl)-pyrimidine[12c] (3.5 mg, 1.3 × 10^{-2} mmol) in 0.7 mL of $CDCl_3$ was stirred at 50 °C for 12 h. The reaction mixture was then concentrated under reduced pressure and purified by flash chromatography (Al_2O_3, $CHCl_3$) to give **42** (9 mg, 60%). Mp > 250 °C (decomposition). ^{1}H NMR: 8.64 (s, 1H), 8.10 (d, ^3J = 4.8 Hz, 2H), 7.97 (s, 2H), 7.91 (s, 2H), 7.85 (d, ^3J = 8.0 Hz, 2H), 7.71 (s, 4H), 7.45 (s, 2H), 7.16 (t, ^3J = 8.0 Hz, 2H), 6.76 (t, ^3J = 4.8 Hz, 2H), 3.84 (s, 6H), 3.61 (s, 6H). ^{13}C NMR: 162.5, 162.1, 161.3, 153.8, 153.1, 149.3, 140.6, 136.1, 135.6, 135.3, 133.4, 132.9, 122.9, 122.1, 119.5, 119.3, 105.5, 87.7, 60.95, 56.3, 55.9, 55.8, 30.2, 29.8. ESI-TOF-MS *m*/*z* (%): 1113.5 (100) [M + H]$^+$.

Crystal Structure of 42 (CCDC 620827). A suitable crystal of **42** was obtained by diffusion−recrystallization from $CHCl_3$ (solvent)/MeOH (nonsolvent). Diffraction data were collected at 173 K. Formula: $C_{60}H_{66}Cl_6N_{16}O_{10}$═$C_{72}H_{62}N_{24}$·2$CHCl_3$·$CH_3OH$. Molecular weight: 1384.01. Yellow crystal; crystal size (mm): 0.20 × 0.10 × 0.10. Unit cell parameters: a = 14.0332 (3) Å, b = 15.6497(3) Å, c = 16.0239(4) Å, α = 87.837(5)°, β = 74.861°(5), γ = 75.625(5)°; crystal system, triclinic; space group P-1; V = 3289.2(1) Å^3; F(000) = 1440; Z = 2; calculated density = 1.40 g cm^{-3}; linear absorption coefficient μ = 0.331 mm^{-1}. Of 27 295 reflections measured, 10 961 reflections were unique ($I > 3\sigma(I)$); 829 refined variables. The θ range for data collection was 2.5−30.05° with *hkl* limits: −19 to 19, −19 to 21, and −22 to 22. The final indices were $R = 0.093$ and $R_w = 0.124$, with a goodness-of-fit (GOF) of 1.068. The largest peak in final difference was 0.776 e Å^{-3}.

Crystal Structure of 43(HOTf)$_2$ (CCDC 620829). A suitable crystal of **43** was obtained by diffusion−recrystallization from $CHCl_3$/TfOH 95:5 (solvent)/MeOH (nonsolvent). Diffraction data were collected at 173 K. Formula: $C_{26}H_{24}F_6N_8O_6S_2$. Molecular weight: 722.65. Colorless crystal; crystal size (mm): 0.20 × 0.20 × 0.20. Unit cell parameters: a = 9.05800 (10) Å, b = 11.4700 (2) Å, c = 29.730 (4) Å, α = 90 °, β = 90°, γ = 90°; crystal system, orthorhombic; space group P_{212121}; V = 3089.12 (8) Å^3; F(000) = 1480; Z = 4; calculated density = 1.554 g cm^{-3}; linear absorption coefficient μ = 0.264 mm^{-1}. Of 8890 reflections measured, 6574 reflections were unique ($I > 2\sigma(I)$); 433 refined variables. The θ range for data collection was 2.35−30.04° with *hkl* limits: −12 to 12, −16 to 16, and −41 to 41. The final indices were $R = 0.0807$ and $R_w = 0.1128$, with a goodness-of-fit (GOF) of 1.008. The largest peak in final difference was 0.316 e Å^{-3}.

4-(Methoxymethyl)-2-phenyl-6-(pyridin-2-yl)pyrimidine (49). A mixture of 4-chloro-6-(methoxymethyl)-2-phenylpyrimidine **39**[12a] (173 mg, 62.6 × 10^{-2} mmol), 2-(trimethylstannyl)pyridine (152 mg, 62.6 × 10^{-2} mmol), and Pd(PPh_3)$_4$ (36.2 mg, 5 mol %) was heated to reflux for 12 h in 6 mL of degassed toluene. After cooling at room temperature, the suspension was dissolved in CH_2Cl_2 and washed consecutively with a saturated solution of potassium fluoride and water, and the organic layers were dried over $MgSO_4$ and purified by flash chromatography (SiO_2, $CHCl_3$/MeOH: 95/5) to give **49** (120 mg, 70%) as a white solid. Mp 94−96 °C. ^{1}H NMR: 8.75 (d, ^3J = 4.0 Hz,1H), 8.70 (d, ^3J = 8.0 Hz, 1H), 8.58 (m, 2H), 8.40 (s, 1H), 7.91 (t, ^3J = 8 Hz, 1H), 7.51 (m,

3H), 7.41 (t, ^3J = 4.8 Hz 1H), 4.70 (s, 2H), 3.58 (s, 3H). ^{13}C NMR: 168.93, 163.88, 163.46, 154.55, 149.73, 137.73, 136.99, 130.62, 128.45, 128.30, 125.24, 121.89, 11.85, 74.82, 59.14. Anal. Calcd for $C_{17}H_{16}N_3O_3$·0.15$CHCl_3$: C, 69.77; H, 5.17; N, 14.23. Found: C, 69.34; H, 5.07; N, 14.97. HRMS (ESi-TOF-MS) *m*/*z* (%): calcd for $C_{17}H_{16}N_3O_1$ 278.1288 $[M + H]^+$; found 278.1282 (100) $[M + H]^+$.

6-(6-(Methoxymethyl)-2-phenylpyrimidin-4-yl)-2,2′-bipyridine (50). A mixture of 4-chloro-6-(methoxymethyl)-2-phenylpyrimidine **39**[12a] (220 mg, 62.6×10^{-2} mmol), 6-(trimethylstannyl)-2,2′-bipyridine[34] (200 mg, 62.6×10^{-2} mmol), and $Pd(PPh_3)_4$ (36.2 mg, 5 mol %) was heated to reflux for 12 h in 6 mL of degassed toluene. After cooling at room temperature, the suspension was dissolved in CH_2Cl_2 and washed consecutively with a saturated solution of potassium fluoride and water, and the organic layers were dried over $MgSO_4$ and purified by flash chromatography (SiO_2, $CHCl_3$/MeOH: 95/5) to afford **50** (135 mg, 61%) as a white solid. Mp 102−104 °C. ^{1}H NMR: 8.71 (m, 2H), 8.64 (d, ^3J = 8.8 Hz, 1H), 8.61 (d, ^3J = 2.4 Hz, 2H), 8.55 (d, ^3J = 8.8 Hz, 1H), 8.52 (s, 1H), 8.00 (t, ^3J = 8.0 Hz, 1H), 7.87 (dt,^{3} J = 7.6 Hz, ^3J = 1.6 Hz, 1H), 7.52 (m, 3H), 7.34 (dd, ^3J = 7.6 Hz, ^3J = 1.2 Hz, 1H), 4.73 (s, 2H), 3.60 (s, 3H). ^{13}C NMR: 168.65, 163.79, 163,47, 155.73, 155.66, 153.69, 149.08, 137.88, 137.69, 136.88, 130.59, 128.45, 128.28, 122.51, 123.89, 122.50, 121.80, 121.25, 111.74, 74.91, 59.09. Anal. Calcd for $C_{17}H_{16}N_3O_3$·0.2$CHCl_3$: C, 70.49; H, 4.85; N, 14.81. Found: C, 70.56; H, 5.01; N, 14.81. HRMS (ESi-TOF-MS) *m*/*z* (%): calcd for $C_{12}H_{19}N_4O_1$ 355.1553 $[M + H]^+$; found 355.1551 (100) $[M + H]^+$.

(2-Phenyl-6-(pyridin-2-yl)pyrimidin-4-yl)methanol (51). A solution of BBr_3 (1 M, 5 mL, in CH_2Cl_2) was added dropwise to a solution of 4-(methoxymethyl)-2-phenyl-6-(pyridin-2-yl)pyrimidine **49** (48 mg, 16.9×10^{-2} mmol) in CH_2Cl_2 (6 mL) at 25 °C. The solution was stirred at the same temperature for 16 h, then cooled to 0 °C and quenched by a slow addition of diethyl ether (1 mL), MeOH (1 mL), and H_2O (1 mL). The mixture was stirred at room temperature for 1 more hour and then extracted with CH_2Cl_2 (2 × 15 mL). The combined organic layers were washed with H_2O (10 mL) and brine (10 mL), dried over Na_2SO_4, filtered, and concentrated to give **51** (40 mg, 90% of crude product). The crude material was used without further purification for the next step. Mp 141−143 °C. ^{1}H NMR: 8.53 (d, ^3J = 4 Hz, 1H), 8.50 (d, ^3J = 7.6 Hz, 1H), 8.38 (m, 2H), 8.13 (s, 1H), 7.79 (t, ^3J = 7.6 Hz, 1H), 7.35 (m, 4H), 4.70 (s, 2H). ^{13}C NMR: 168.90, 163.88, 163.46, 154.44, 149.47, 137.73, 136.99, 130.62, 128.48, 128.30, 125.24, 121.89, 111.85, 74.82. HRMS (ESi-TOF-MS) *m*/*z* (%): calcd for $C_{16}H_{13}Li_1N_3O_1$ 270.1213 $[M + Li]^+$; found 270.1211 (100) $[M + Li]^+$.

(6-(2,2′-Bipyridin-6-yl)-2-phenylpyrimidin-4-yl)methanol (52). A solution of BBr_3 (1 M, 5 mL, in CH_2Cl_2) was added by syringe to a solution of 6-(6-(methoxymethyl)-2-phenylpyrimidin-4-yl)-2,2′-bipyridine **50** (60 mg, 16.9×10^{-2} mmol) in CH_2Cl_2 (6 mL) at 25 °C. The solution was stirred at 25 °C for 16 h, and was then cooled to 0 °C and quenched by slow addition of diethyl ether (1 mL), MeOH (1 mL), and H_2O (1 mL). The mixture was stirred at room temperature for 1 more hour and then extracted with CH_2Cl_2 (2 × 15 mL). The combined organic layers were washed with H_2O (10 mL) and brine (10 mL), dried over Na_2SO_4, filtered, and concentrated to give **52** (55 mg, 95%) as a white solid. The crude material was used without further purification for the next step. ^{1}H NMR: 8.71 (m, 2H), 8.58 (m, 4H), 8.35 (s, 1H), 8.01 (t, ^3J = 8 Hz, 1H), 7.88 (td, ^3J = 7, 6 Hz, ^3J = 2 Hz, 1H), 7.53 (m, 3H), 7.35 (dd, ^3J = 8 Hz, ^3J = 1.2 Hz, 1H), 4.94 (s, 2H). ^{13}C NMR: 169.02, 163.37, 162.89, 155.59, 155.53, 153.20, 149.08, 137.89, 137.18, 136.90, 130.82, 128.46, 128.24, 123.93, 122.64, 121.81, 121.20, 111.10, 63.98. Anal. Calcd for $C_{21}H_{16}N_4O$·0.2$CHCl_3$: C, 69.90; H, 4.48; N, 15.38. Found: C, 70.23; H, 4.74; N, 15.49. HRMS (ESi-TOF-MS) *m*/*z* (%): calcd for $C_{21}H_{17}N_4O_1$ 341.1397 $[M + H]^+$; found 341.1391 (100) $[M + H]^+$.

6-(2,2′-Bipyridin-6-yl)-2-phenylpyrimidine-4-carbaldehyde (53). To a solution of (6-(2,2′-bipyridin-6-yl)-2-phenylpyrimidin-4-yl)methanol **52** (55 mg, 16×10^{-2} mmol) in CH_2Cl_2 (20 mL) was added Dess−Martin reagent (140 mg, 32×10^{-2} mmol). After 6 h of stirring, the reaction mixture was quenched using 50 mL of a saturated solution of $NaHCO_3$ (50 mL). The organic layer was dried over Na_2SO_4, filtered, and concentrated. The crude material was purified by flash chromatography (SiO_2, $CHCl_3$/MeOH: 96/4) to give **53** (45 mg, 83%) as a yellow solid. Mp 182−184 °C. ^{1}H NMR: 10.23 (s, 1H), 8.87 (s, 1H), 8.68 (m, 5H), 8.61 (d, ^3J = 7.2 Hz, 1H), 8.04 (t, ^3J = 8 Hz, 1H), 7.91 (td, ^3J = 8 Hz, ^3J = 2 Hz, 1H), 7.56 (m, 3H), 7.37 (dd, ^3J = 7.6 Hz, ^3J = 1.2 Hz, 1H). ^{13}C NMR: 193.46, 165.32, 165.14, 159.25, 155.87, 155.24, 152.54, 148.98, 137.92, 136.88, 136.65, 131.18, 128.53, 128.28, 123.95, 122.98, 121.66, 121.17, 110.70. HRMS (ESi-TOF-MS) *m*/*z* (%): calcd for $C_{21}H_{14}Li_1N_4O_1$ 345.1322 $[M + Li]^+$; found 345.1322 (100) $[M + Li]^+$.

2-Phenyl-6-(pyridin-2-yl)pyrimidine-4-carbaldehyde (54). To a solution of (2-phenyl-6-(pyridin-2-yl)pyrimidin-4-yl)methanol **51** (25 mg, 0.095 mmol) in CH_2Cl_2 (6 mL) was added Dess−Martin reagent (80 mg, 1.9 mmol). After 6 h of stirring, the reaction mixture was quenched using 50 mL of a saturated solution of $NaHCO_3$ (50 mL). The organic layer was dried over Na_2SO_4, filtered, and concentrated. The crude material was purified by flash chromatography (SiO_2, $CHCl_3$/MeOH: 96/4) to give **54** (12 mg, 48%) as a white solid. Mp 129−131 °C. ^{1}H NMR: 10.22 (s, 1H), 8.78 (d, ^3J = 4.8 Hz, 1H), 8.87 (s, 1H), 8.04 (d, ^3J = 7.2 Hz, 1H), 8.66 (m, 3H), 7.37 (t, ^3J = 7.6 Hz, 1H), 7.57 (m, 3H), 7.37 (t, ^3J = 7.2 Hz, 1H). ^{13}C NMR: 193.28, 165.53, 15955, 149.76, 137.13, 136.81, 131.37, 128.73, 128.48, 125.86, 121.96, 111.18. HRMS (ESi-TOF-MS) *m*/*z* (%): calcd for $C_{16}H_{12}N_3O_1$ 262.0975 $[M + H]^+$; found 262.0968 (100) $[M + H]^+$.

(1-Methyl-2-(pyridin-2-ylmethylene)hydrazinyl)-2-phenylpyrimidine-4-methanol (55). A solution of **38** (50 mg, 0.22 mmol) and pyridine-2-carboxaldehyde (23.3 mg, 0.22 mmol) was stirred in 5 mL of absolute ethanol at room temperature for 4 h under an argon atmosphere. The solution was then concentrated under reduced pressure and filtered to give **40** (56 mg, 80%) as a white solid. ^{1}H NMR (DMSO-d_6): 8.64 (d, ^3J = 4.4 Hz, 1H), 8.43 (m, 2H), 8.04 (d, ^3J = 8.0 Hz, 1H), 8.00 (s, 1H), 7.71 (s, 1H), 7.52 (m, 3H), 7.40 (t, ^3J = 8 Hz 1H), 7.71 (t, ^3J = 4.4 Hz,1H), 4.60 (d, 2H), 3.82 (s, 3H). ^{13}C NMR (DMSO-d_6): 171.2, 163.12, 162.17, 154.4, 149.9, 139.4, 137.8, 137.2, 130.9, 128.8, 128.2, 124.0, 119.9, 100.1, 64.30, 29.89. Anal. Calcd for $C_{18}H_{17}N_5O$: C, 67.70; H, 5.37; N, 21.93. Found: C, 67.59; H, 5.15; N, 22.15. ESI-TOF-MS *m*/*z* (%): 320.14(100) $[M + H]^+$.

Crystal Structure of 55 (CCDC 620828). A suitable crystal of **55** was obtained by diffusion−recrystallization from $CHCl_3$ (solvent). Diffraction data were collected at 173 K. Formula: $C_{18}H_{17}N_5O$. Molecular weight: 319.37. Yellow crystal; crystal size (mm): 0.20 × 0.10 × 0.10. Unit cell parameters: a = 8.3996 (3) Å, b = 13.3132 (3) Å, c = 14.1796 (4) Å, α = 90(5)°, β = 90(5)°, γ = 90(5)°; crystal system, orthorhombic; space group P_{212121}; V = 1585.64(1) Å^3; F(000) = 672; Z = 4; calculated density = 1.34 g cm^{-3}; linear absorption coefficient μ = 0.088 mm^{-1}. Of 4581 reflections measured, 2981 reflections were unique ($I > 3\sigma(I)$); 217 refined variables. The θ range for data collection was 2.5−30.02° with *hkl* limits: −11 to 11, −18 to 18, and −19 to 19. The final indices were R = 0.042 and R_w = 0.055, with a goodness-of-fit (GOF) of 1.037. The largest peak in final difference was 0.831 e Å^{-3}.

(1-Methyl-2-(pyridin-2-ylmethylene)hydrazinyl)-2-phenylpyrimidine-4-carbaldehyde (56). A solution of Dess−Martin reagent (15% in CH_2Cl_2, 7.1 g) was added to a solution of **55** (800 mg, 2.51 mmol) in CH_2Cl_2 (60 mL), and the reaction was stirred for 6 h. Dichloromethane (100 mL) and a saturated aqueous solution of $NaHCO_3$ (50 mL) were added, and the aqueous layer was extracted with CH_2Cl_2 (2 × 50 mL). The combined organic layers were dried over Na_2SO_4, filtered, and concentrated under vacuum. The crude material was purified by flash chromatography (SiO_2, $CHCl_3$/MeOH: 96/4) to give **56** (220 mg, 30%) as a yellow solid. ^{1}H NMR: 10.14 (s, 1H), 8.66 (d, ^3J = 4.4 Hz, 1H), 8.55 (m, 2H), 8.19 (d, ^3J = 8.0 Hz, 1H), 8.06 (s,

(34) Cardenas, D. J.; Sauvage, J.-P. *Synlett* **1996**, 916.

1H), 8.05 (s, 1H), 7.84 (t, ^3J = 8.0 Hz, 1H), 7.55 (m, 3H), 7.31 (dd, ^3J = 4.4 Hz, ^3J = 4.4 Hz, 1H), 2.89 (s, 3H). ^{13}C NMR: 193.9, 164.6, 163.7, 158.3, 153.9, 149.2, 139.6, 136.9, 131.1, 128.5, 128.2, 123.7, 120.2, 112.6, 110.0, 101.3, 29.7. FAB-MS *m*/*z* (%): 318.1 (100) [M + H]$^+$.

6-(6-((*E*)-(2-Methyl-2-(6-((*E*)-1-methyl-2-((6-((*E*)-(2-methyl-2-(6-((*E*)-1-methyl-2-(pyridin-2-ylmethylene)hydrazinyl)-2-(3,4,5-trimethoxyphenyl)pyrimidin-4-yl)hydrazono)methyl)-2-phenylpyrimidin-4-yl)methylene)hydrazinyl)-2-(3,4,5-trimethoxyphenyl)pyrimidin-4-yl)hydrazono)methyl)-2-phenylpyrimidin-4-yl)-2,2′-bipyridine (57). A solution of **34** (60 mg, 0.091 mmol) and **35** (56.6 mg, 0.091 mmol) in 1.5 mL of $CDCl_3$ was stirred at 30 °C for 1 h. The solution was then concentrated under reduced pressure and purified by flash chromatography (Al_2O_3, $CHCl_3$) to give **55** (40 mg, 35%) as a yellow powder. Mp > 250 °C (decomposition). ^{1}H NMR: 8.96 (s, 1H), 8.64 (d, ^3J = 7.6 Hz, 2H), 8.50 (d, ^3J = 7.2 Hz, 2H), 8.37 (m, 2H), 8.30 (m, 3H), 8.24 (s, 1H), 8.18 (d, ^3J = 3.8 Hz, 1H), 8.12 (l, 1H), 8.05 (t, ^3J = 7.8 Hz, 1H), 7.90−7.50 (m, 5H), 7.66 (s, 1H), 7.63−7.58 (m, 3H), 7.41 (s, 2H), 7.39−7.25 (m, 4H), 7.20 (t, ^3J = 7.8 Hz, 2H), 7.07 (s, 1H), 6.93 (t, ^3J = 4.7 Hz, 1H), 6.73 (l, 1H), 4.11 (s, 6H), 4.02 (s, 3H), 4.01 (s, 3H), 3.94 (s, 3H), 3.92 (s, 6H), 3.83 (s, 3H), 3.74 (s, 3H), 3.40 (s, 3H). ^{13}C NMR: 161.40, 160.95, 160.90, 155.30, 154.80, 153.55, 153.15, 152.55, 148.50, 140.50, 140.00, 137.75, 137.35, 137.00, 136.55, 136.05, 135.75, 134.85, 133.35, 133.10, 130.40, 130.25, 128.50, 128.25, 127.90, 127.80, 123.50, 122.25, 122.05, 121.15, 120.65, 109.05, 107.05, 105.45, 105.05, 97.95, 88.05, 86.95, 61.00, 60.85, 56.30, 55.90, 30.30, 30.00, 29.40. HRMS (ESi-TOF-MS) *m*/*z* (%): calcd for $C_{68}H_{60}N_{19}O_7$ 1254.5281 [M + H]$^+$; found 1254.5079 (100) [M + H]$^+$.

Acknowledgment. We thank Dr. Patrick Wehrung for assistance with mass spectroscopy and also Dr. André de Cian and Dr. Augustin Madalan for help with X-ray diffraction radiocrystallography.

Supporting Information Available: Crystallographic data (CIF). This material is available free of charge via the Internet at http://pubs.acs.org.

JA0666452